

000 001 002 003 004 005 006 007 008 009 010 011 012 013 014 015 016 017 018 019 020 021 022 023 024 025 026 027 028 029 030 031 032 033 034 035 036 037 038 039 040 041 042 043 044 045 046 047 048 049 050 051 052 053 EXPANDING THE CAPABILITY FRONTIER OF LLM AGENTS WITH ZPD-GUIDED DATA SYNTHESIS

Anonymous authors

Paper under double-blind review

ABSTRACT

Unlocking advanced reasoning in large language model agents is hindered by a scarcity of training data situated at the very frontier of their capabilities. We address this with a novel data synthesis approach inspired by the educational theory of the Zone of Proximal Development (ZPD), which conceptualizes this frontier as tasks an LLM cannot solve independently but can master with guidance. We operationalize this principle through the **AgentFrontier Data Engine**, an automated pipeline that synthesizes high-quality, multidisciplinary data situated precisely within an LLM’s ZPD. The engine yields two synergistic outputs: knowledge-intensive data for continued pre-training and frontier-level reasoning trajectories for post-training. Concurrently, it produces the **ZPD Exam**, a self-evolving benchmark for evaluating agent capabilities by compelling them to reason beyond their parameterized knowledge. By training our **AgentFrontier-30B-A3B** model on the synthesized data, we achieve state-of-the-art results on demanding benchmarks like *Humanity’s Last Exam*, outperforming several leading proprietary agents. This work establishes ZPD-guided data synthesis as a scalable and effective paradigm for cultivating increasingly capable LLM agents.

1 INTRODUCTION

While large language models (LLMs) have demonstrated impressive proficiency on various fundamental reasoning tasks (Rein et al., 2023; Wang et al., 2024; Tian et al., 2024), they still struggle with the scenarios demanding in-depth, cross-domain, and integrative reasoning (Mialon et al., 2023; Wei et al., 2025; Phan et al., 2025). This gap presents a critical impediment in the pursuit of artificial general intelligence (AGI). Achieving such a leap necessitates a paradigm shift from reliance on static, internal knowledge to dynamic, agentic capabilities such as tool using (Qin et al., 2024), self-reflection (Shinn et al., 2023), iterative planning, and multi-step reasoning. However, the development of such agentic skills is hampered by a dual challenge: a scarcity of training corpora that systematically cultivate these abilities in a unified manner (Shi et al., 2025), and the saturation of existing benchmarks. While expert-crafted evaluations such as *Humanity’s Last Exam* (Phan et al., 2025) offer invaluable benchmarks, their prohibitive cost and limited scalability underscore the urgent need for automated pipelines capable of synthesizing frontier-level reasoning tasks.

Recent datasets have significantly enhanced LLMs’ single-step reasoning (Liu et al., 2025), but they fall short of targeting the deeper challenge of **knowledge fusion** (Wan et al., 2024): integrating and transforming information across diverse sources. While retrieval-augmented generation (RAG) (Lewis et al., 2020) excels when the answer can be grounded in a single document, its performance degrades on tasks requiring reasoning across heterogeneous information. This deficiency traces back to the dominant data-synthesis paradigms, which fall into two broad categories: query-centric methods (Yan et al., 2025) that generate variations of existing question–answer (QA) pairs, and document-centric methods (Fan et al., 2025; Yuan et al., 2025) that derive document-grounded QA pairs from the corpus. Both approaches primarily assess localized comprehension, akin to examining a student on individual textbook chapter rather than their ability to synthesize insights across an entire curriculum. In contrast, complex real-world tasks such as academic research, legal analysis, or engineering design demand multi-document synthesis and cross-domain knowledge fusion. Human experts rarely treat information in isolation; instead, they connect, contrast, and integrate it to derive in-depth insights, which is the intrinsic essence of **deep research** (OpenAI, 2025a; Google, 2025).

054 Cultivating such synthetic reasoning capacity is paramount to advancing LLMs toward higher forms
 055 of intelligence.
 056

057 The central challenge of effective data synthesis lies not in
 058 merely generating difficult tasks, but in precisely calibrating
 059 them to the frontier of a model’s competence: complex enough
 060 to exceed the boundary of the model’s intrinsic capability, yet
 061 solvable with appropriate support. Existing approaches typi-
 062 cally rely on coarse-grained difficulty annotations (Su et al.,
 063 2025) or heuristically stacked constraints (Patel et al., 2025),
 064 lacking a precise mechanism for targeting this frontier. In
 065 practice, self-generated approaches tend to yield data confined
 066 within the model’s own expressive ceiling, thus hindering sys-
 067 tematic difficulty progression. To address this, we draw inspi-
 068 ration from the educational psychology concept of the **Zone**
 069 of **Proximal Development** (ZPD) (Vygotsky, 1978; McLeod,
 070 2012), which defines the cognitive space where a learner can
 071 succeed with guidance on tasks they cannot solve alone. We
 072 operationalize this by defining two personas: the **Less Knowl-
 073 edgeable Peer** (LKP), a base LLM, and the **More Knowl-
 074 edgeable Other** (MKO), a superior tool-augmented agent with ad-
 075 vanced reasoning. By definition, tasks that the LKP fails but the
 076 MKO masters are situated within the model’s ZPD. This provides a
 077 principled mechanism for identifying maximally informative training
 078 resources and, crucially, allows for a continuously adaptive curricu-
 079 lum that evolves as the model’s own capability frontier expands.
 080

081 We instantiate this principle in the **AgentFrontier Engine**, a novel data synthesis framework de-
 082 signed to generate complex-reasoning data within LLM’s ZPD. The engine operates via a process
 083 of adversarial calibration, dynamically probing the capability frontier of the LLMs. It constructs
 084 multi-disciplinary QA pairs that necessitate knowledge fusion across multiple web sources, mov-
 085 ing beyond simple fact retrieval. Our engine employs a dual-pipeline architecture: tasks solvable
 086 by the LKP are curated as knowledge-intensive data for continued pre-training (CPT), while those
 087 requiring the MKO are designated as frontier-level data for post-training. This design establishes a
 088 virtuous cycle, yielding a continuous stream of adaptive data that propels model capability forward.
 089

090 Our contributions are threefold:
 091

- 092 1. We present **AgentFrontier Engine**, a scalable data synthesis framework founded on the
 093 theory of *Zone of Proximal Development* (ZPD). By integrating agentic refinement and
 094 LKP–MKO adversarial calibration, it generates a dual stream of knowledge-intensive data
 095 for broad competence and frontier-level data for advanced reasoning.
- 096 2. We establish **ZPD Exam**, an automated benchmark designed to probe the ZPD of LLMs. It
 097 assesses advanced capabilities such as tool using and in-depth reasoning by complex multi-
 098 disciplinary questions that require cross-document knowledge fusion and deep research.
- 099 3. We demonstrate the effectiveness of our framework by developing **AgentFrontier-30B-A3B**. By applying continued pre-training on 50 billion tokens of knowledge-intensive data
 100 and fine-tuning on 12,000 frontier-level trajectories synthesized by our engine, the result-
 101 ing model achieves 28.6% on the challenging HLE benchmark and sets state-of-the-art
 102 performance on ZPD Exam-v1, R-Bench-T and xBench-ScienceQA.

2 AGENTFRONTIER DATA ENGINE

103 **AgentFrontier Engine** addresses the critical need for training data that fosters knowledge fusion
 104 and complex reasoning, which operationalizes the theoretical framework of the *Zone of Proximal*
 105 *Development* to generate challenging tasks that reside at the frontier of a LLM’s capabilities. In-
 106 stead of passively curating existing information, the engine is designed to actively forge complexity
 107 through a three-stage agentic synthesis pipeline. This process aims to evolve LLMs from knowledge
 108 retrievers into sophisticated reasoning agents. The entire workflow, depicted in Figure 2, transforms
 109 a raw document corpus C_{raw} into a calibrated, high-value dataset \mathcal{D}_{ZPD} . The detailed procedure is
 110 presented in Algorithm 1. The detailed prompts are provided in the Appendix F.

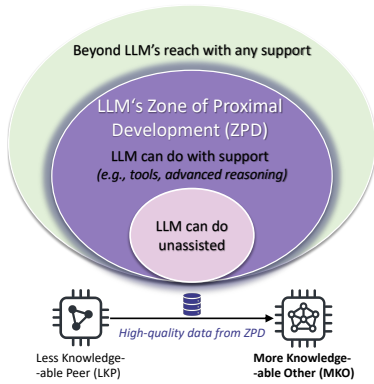


Figure 1: High-quality data within an LLM’s ZPD catalyzes its transformation from LKP to MKO.

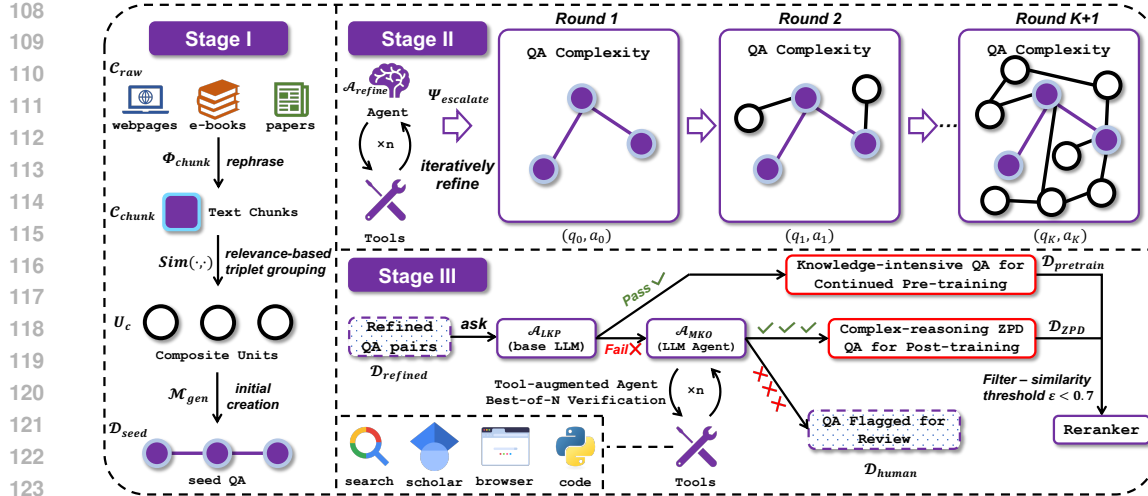


Figure 2: The three-stage pipeline of the AgentFrontier Engine. Stage I generates seed QA pairs from multiple sources. Stage II iteratively escalates their complexity using a tool-augmented agent. Stage III applies a ZPD-based calibration filter to isolate high-value training samples.

2.1 STAGE I: SEED QUESTION GENERATION FOR KNOWLEDGE FUSION

The pipeline begins with a diverse, multi-disciplinary corpus C_{raw} of one million public documents. We first employ a powerful LLM, Qwen3-235B-A22B (Yang et al., 2025), as a chunking function Φ_{chunk} to preprocess the corpus. This function cleans artifacts (e.g., HTML tags) and condenses long texts into information-dense chunks C_{chunk} , such that $C_{\text{chunk}} = \bigcup_{d \in C_{\text{raw}}} \Phi_{\text{chunk}}(d)$.

To generate tasks that inherently demand knowledge fusion, we synthesize questions from **composite units**—groups of thematically related chunks. To overcome the computational infeasibility of a combinatorial search, we adopt an efficient, retrieval-based approach. We first build a vector index over C_{chunk} and, for each chunk c_i , retrieve its k_{nn} nearest neighbors. Within this local neighborhood, we search for triplets (c_i, c_j, c_k) that exhibit high thematic coherence, formally defined as $\text{Sim}(c_x, c_y) > \tau_{\text{theme}}$ for all distinct pairs, where $\text{Sim}(\cdot, \cdot)$ is a semantic similarity function.

These composite units are then fed to a generator model, M_{gen} (DeepSeek-R1-0528 (Guo et al., 2025a)), to synthesize initial question-answer pairs. This process yields a seed dataset that serves as the foundation for complexity escalation: $\mathcal{D}_{\text{seed}} = \{(q_0, a_0) = M_{\text{gen}}(U_c) \mid U_c \text{ is a composite unit}\}$.

2.2 STAGE II: ESCALATING COMPLEXITY THROUGH AGENTIC REFINEMENT

The core of our engine is an iterative refinement loop driven by a refinement agent A_{refine} , which integrates DeepSeek-R1 with a tool suite $\mathcal{T} = \{T_{\text{search}}, T_{\text{scholar}}, T_{\text{browser}}, T_{\text{code}}\}$. For a QA pair (q_k, a_k) at iteration k , the agent applies an escalation operator Ψ_{escalate} to generate a more sophisticated pair $(q_{k+1}, a_{k+1}) = \Psi_{\text{escalate}}(q_k, a_k, A_{\text{refine}})$. This operator enriches the QA along four dimensions:

- **Knowledge Expansion:** It actively queries external sources to retrieve and weave in relevant background knowledge, broadening the informational scope of the question.
- **Conceptual Abstraction:** It conducts in-depth analysis of the core concepts within the provided materials, abstracting higher-level principles or identifying subtle relationships.
- **Factual Grounding:** It performs multi-source cross-validation and targeted augmentation to enhance the factual accuracy and depth of the content.
- **Computational Formulation:** It leverages the Python execution to craft QA that require quantitative calculation or logical simulation, assessing reasoning and computational skills.

This self-bootstrapping process creates a virtuous cycle, where the output of one iteration becomes the input for the next, building increasingly more intricate reasoning paths. Figure 6 illustrates an example where a question is progressively refined by interleaving web search with numerical computation. After K iterations, this stage produces a dataset of highly complex QA pairs, $\mathcal{D}_{\text{refined}}$.

162 2.3 STAGE III: ZPD-BASED FILTERING AND CALIBRATION
163

164 Not all synthesized QA pairs are equally valuable for training. To isolate tasks that reside precisely
165 within an LLM’s ZPD, we introduce a rigorous calibration mechanism based on our **LKP-MKO**
166 framework. We instantiate a **Less Knowledgeable Peer** (\mathcal{A}_{LKP}) with the base DeepSeek-R1-0528
167 model (without tools) (Guo et al., 2025a) and a **More Knowledgeable Other** (\mathcal{A}_{MKO}) with the
168 powerful, tool-augmented DeepSeek-V3.1 agent (Liu et al., 2024).

169 For each candidate pair $(q, a) \in \mathcal{D}_{\text{refined}}$, we first assess its difficulty. Let $\text{IsSolvableBy}(\mathcal{A}, q, a) \in$
170 $\{0, 1\}$ be a binary function, implemented by an automated judge (GPT-4o (OpenAI, 2024)), which
171 returns 1 if agent \mathcal{A} correctly answers q . (a) If $\text{IsSolvableBy}(\mathcal{A}_{\text{LKP}}, q, a) = 1$, the pair is deemed
172 too simple and is allocated to a general knowledge dataset $\mathcal{D}_{\text{pretrain}}$ for continued pre-training. (b) If
173 $\text{IsSolvableBy}(\mathcal{A}_{\text{LKP}}, q, a) = 0$, the pair is challenging and passed to the MKO for further evaluation.

174 To stratify the challenging data, \mathcal{A}_{MKO} performs Best-of-N (BoN) verification with $N = 3$, generating
175 N independent solutions $\{s_1, \dots, s_N\}$. The data is then partitioned based on the outcome:
176

- 177 • **Verified for Post-Training** (\mathcal{D}_{ZPD}): If the MKO finds at least one correct solution
178 (i.e., $\sum_{i=1}^N \text{IsCorrect}(s_i, a) \geq 1$), the pair is considered to be within the model’s
179 ZPD—challenging yet learnable. These verified pairs form our final training set.
- 180 • **Flagged for Human Review** ($\mathcal{D}_{\text{human}}$): If the MKO fails in all N attempts (i.e.,
181 $\sum_{i=1}^N \text{IsCorrect}(s_i, a) = 0$), the pair is either flawed or exceptionally difficult and is routed
182 to human experts for analysis. [The human review process is detailed in the Appendix C.4](#).

184 Finally, to ensure dataset diversity, we apply a semantic redundancy filter. A newly generated
185 pair (q', a') is discarded if its question q' is too similar to any question already in \mathcal{D}_{ZPD} . Specifically,
186 we discard (q', a') if $\max_{(q, a) \in \mathcal{D}_{\text{ZPD}}} \text{Sim}(q', q) \geq \epsilon$, where $\text{Sim}(\cdot, \cdot)$ is measured by a reranker
187 model (Zhang et al., 2025) and the threshold ϵ is set to 0.7.

188 Through this three-stage pipeline, the AgentFrontier Engine provides a scalable method for generating
189 complex reasoning data, continuously pushing the boundaries of LLM capabilities.
190

191 3 ZPD EXAM: A SELF-EVOLVING BENCHMARK FOR LLM AGENTS
192

193 Evaluating rapidly advancing LLMs requires benchmarks that co-evolve with their capabilities.
194 While expert-crafted exams like Humanity’s Last Exam (Phan et al., 2025) probe the frontier of
195 human knowledge, their static nature and prohibitive creation costs hinder scalable and continuous
196 assessment. We introduce the **ZPD Exam**, an automated and continuously evolving benchmark
197 designed to assess the deep research capabilities of advanced LLM agents.
198

199 3.1 BENCHMARK CONSTRUCTION: FROM FRONTIER KNOWLEDGE TO AGENTIC RESEARCH
200

201 The ZPD Exam is designed to simulate scientific discovery by generating tasks that are intractable
202 using only parametric knowledge, thus compelling models to function as research agents. The
203 benchmark is constructed using our AgentFrontier Engine (Section 2), specifically configured to
204 generate novel, multi-disciplinary questions. Crucially, this benchmark corpus is strictly disjoint
205 from the corpus used to construct our training data, ensuring a fair and uncontaminated evaluation.

206 **Grounding in the Knowledge Frontier.** We ground this exam in the knowledge frontier by curating
207 a corpus of 30,000 recent scientific papers published between 2023 and 2025, spanning multi-
208 disciplinary domains such as mathematics, computer science, and physics. This ensures that success
209 demands genuine, on-the-fly reasoning and information synthesis, not merely knowledge retrieval.

210 **Calibrating Tasks to the LLM’s ZPD.** From our initial corpus, the AgentFrontier Engine generates
211 candidate questions, which are then subjected to a strict adversarial filter to align with the ZPD of
212 a baseline model (DeepSeek-R1-0528 (Guo et al., 2025a)). To be included in ZPD Exam-v1, a
213 problem must satisfy a dual constraint: it must be unsolvable by the baseline model in three unaided
214 attempts, yet consistently solvable by the same model across three attempts when granted access
215 to tools. This process isolates problems that are difficult but solvable with assistance, defining the
empirical boundary of the model’s ZPD.

This automated pipeline enables a flywheel-like iterative process: as models improve, the ZPD exam can be regenerated to target the new frontier, making it a **living benchmark** resistant to saturation. After multiple rounds of validation and deduplication, ZPD Exam-v1 was constructed by sampling 1,024 public questions and a corresponding private set. All questions are open-ended short-answer format, facilitating automated grading. The benchmark composition is detailed in Figure 7.

3.2 ZPD EXAM: A DIAGNOSTIC BENCHMARK FOR AGENTIC REASONING

The ZPD Exam proposes a new evaluative framework, shifting the focus from an LLM’s static parametric knowledge (Hendrycks et al., 2021) to its dynamic capacity for knowledge discovery, which functions as an “open-book” examination where agent must first author the “book” through active exploration and tool use. This design philosophy deliberately situates the challenges within the ZPD for current LLMs, a calibration confirmed by their low initial scores (Figure 3). Our empirical results validate this diagnostic power, revealing a clear stratification of agent performance into three distinct zones.

Zone 1: Intrinsic Competence (Score < 20). This tier establishes the baseline, reflecting the performance of LLMs relying solely on their parametric knowledge (e.g., GPT-5 and Gemini-2.5-Pro without tools). By design, the problems are intractable without external information, confirming that these tasks lie outside the models’ unaided capabilities. This zone effectively establishes a baseline, quantifying the limits of intrinsic, “closed-book” reasoning, confirming that any score above this threshold is directly attributable to the agent’s ability to leverage external tools support.

Zone 2: The Reasoning Bottleneck (Score 20-60). This intermediate tier characterizes the ZPD itself, where agents (e.g., GPT-4o with tools, WebShaper-72b) can achieve partial success with assistance but lack mastery. This zone highlights the benchmark’s crucial distinction from standard RAG evaluations. While RAG tests comprehension of a given context, agents here falter in the more demanding task of autonomously discovering, structuring, and reasoning over the necessary information. Their failures stem not from tool-level errors but from a higher-order “reasoning bottleneck”: a deficit in strategic planning, synthesizing information across multiple tool calls, and adapting their approach. This reveals that access to tools is necessary but insufficient; the primary limiting factor is the agent’s meta-cognitive ability to orchestrate these tools effectively.

Zone 3: Emergent Mastery (Score > 60). Agents in this top tier (e.g., DeepSeek-V3.1 with tools) demonstrate a qualitative leap in capability. They have transcended the reasoning bottleneck and exhibit robust, multi-step planning and synthesis. Their behavior is analogous to the More Knowledgeable Other, seamlessly integrating tool-based exploration into a coherent reasoning process to solve problems far beyond their intrinsic reach. Achieving this level of performance signifies the emergence of a truly capable agent that can autonomously navigate complex problem spaces.

In summary, the ZPD Exam serves not merely as a leaderboard but as a powerful diagnostic instrument. Its tiered results provide a fine-grained analysis of an agent’s developmental stage—from what it knows (intrinsic), to what it can learn to do with support (ZPD), to what it has mastered. This allows us to pinpoint critical reasoning faculties that require improvement, thereby charting a clear path toward more autonomous and capable AI agents.

4 EXPERIMENTS

4.1 EXPERIMENTAL SETUP

Training Data Synthesis. We synthesize training trajectories using a tool-augmented DeepSeek-V3.1 (Liu et al., 2024), following the iterative tool-calling and summarization paradigm from We-

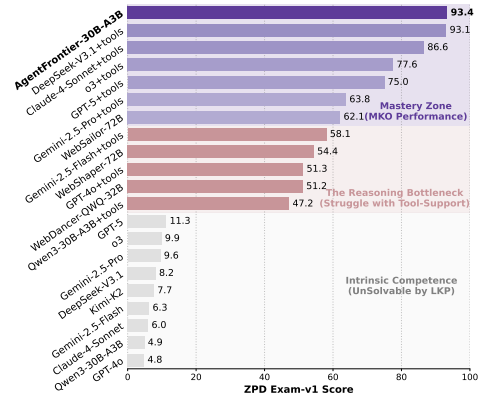


Figure 3: Performance of LLM agents on the ZPD Exam-v1 benchmark, stratified into three distinct capability zones.

bResearcher (Qiao et al., 2025). Each trajectory is generated through a multi-round process adhering to the ReAct (Yao et al., 2023), comprising a sequence of round-wise reasoning reports and observations after the corresponding tool calls. In each round, the model generates a reasoning report that summarizes accumulated evidence, analyzes progress towards the research question, and specifies the next action—either invoking a new tool or outputting a final answer.

Baselines and Fine-Tuning. We compare our proposed AgentFrontier dataset against three prominent, multi-disciplinary agent-tuning datasets: TaskCraft (Shi et al., 2025), MegaScience (Fan et al., 2025) and MiroVerse (MiroMind-Data-Team, 2025). To ensure a fair comparison, we first curate a high-quality subset of 12,000 trajectories for each dataset via rejection sampling, retaining only instances where the final answer is perfectly correct. As shown in Table 1, our AgentFrontier dataset exhibits a more balanced and diverse tool-use distribution compared to the baselines, with substantial usage across scholar, browser, and code tools. This reflects its focus on complex reasoning problem-solving. For rejection sampling fine-tuning (RFT), we normalize the training data volume to 25,600 rounds for each dataset, with each round capped at 40,960 tokens, and train for 3 epochs.

Models and Evaluation. We conduct experiments on the Qwen3 model family (Yang et al., 2025), including both dense (Qwen3-8B, Qwen3-32B) and Mixture-of-Experts (Qwen3-30B-A3B-Thinking-2507) variants. We evaluate performance on four challenging benchmarks designed to probe high-level reasoning across diverse disciplines: HLE (Phan et al., 2025), ZPD Exam, R-Bench (Guo et al., 2025b) and xBench-ScienceQA (Xbench-Team, 2025). For evaluating the correctness of final answers, we employ an **LLM-as-a-Judge**. Specifically, we use o3-mini (OpenAI, 2025b) as the judge, guided by the official strict evaluation prompt from HLE (Phan et al., 2025). All model generations use nucleus sampling with a temperature of 0.6 and a top-p of 0.95.

4.2 MAIN RESULTS

Overall Performance Across Benchmarks. Table 2 illustrates the performance of the Qwen3-series models after fine-tuning. Models trained on AgentFrontier consistently achieve state-of-the-art results, decisively outperforming all baseline datasets across all four benchmarks. In contrast, the performance of competing datasets such as TaskCraft (Shi et al., 2025), MegaScience (Fan et al., 2025), and MiroVerse (MiroMind-Data-Team, 2025) is inconsistent; while each may show strength on a particular benchmark, none demonstrates the robust, cross-domain superiority imparted by AgentFrontier. This trend of superior and consistent performance holds across other model backbones as well.

Subject-Level Dominance on the HLE Benchmark. To investigate the source of this performance advantage, we conduct a fine-grained analysis on the particularly demanding Humanity’s Last Exam (HLE) (Phan et al., 2025) benchmark, examining results across eight academic disciplines with various model backbones (Table 3). For both the Qwen3-8B and Qwen3-32B backbones, models trained on AgentFrontier exhibit remarkable breadth, securing the top performance in six and seven out of the eight subjects, respectively. This subject-level dominance translates to a significant lead in overall average scores, with AgentFrontier surpassing the next-best dataset by 3.8 and 3.9 absolute points on the 8B and 32B models, respectively. The advantage becomes even more pronounced with the Qwen3-30B-A3B model, where fine-tuning on AgentFrontier outperforms all competing datasets in every single subject. This comprehensive superiority results in a final average score of 25.67%, representing a 178% and 152% relative improvement over the original base model in settings without and with tool augmentation, respectively. These results indicate that as model capacity increases, the rich, multi-step reasoning trajectories within AgentFrontier become increasingly effective at unlocking expert-level problem-solving capabilities across a wide spectrum of academic fields.

Table 1: Statistics of trajectories across the training datasets. Avg. Rounds and Avg. Calls are computed per trajectory.

Dataset	Rounds	Avg. Tool Calls			
		Search	Scholar	Browser	Code
TaskCraft	3.38	1.04	0.14	1.19	0.01
MegaScience	2.68	0.26	0.56	0.49	0.37
MiroVerse	2.18	0.12	0.04	0.09	0.93
AgentFrontier	3.32	0.32	0.66	0.82	0.52

324
325 Table 2: Performance comparison on four multi-disciplinary benchmarks. Scores are reported as
326 "mean \pm confidence interval". The **best** score is highlighted, and the second-best is underlined.
327

328 RFT Dataset	329 Tools	330 Evaluation on Four Multi-disciplinary Benchmarks			
		331 HLE (text-only)	332 ZPD Exam-v1	333 RBench-T	334 xBench-SciQA
<i>335 Backbone: Qwen3-8B</i>					
336 \neg (no-finetuning)	337 \times	338 4.0 ± 0.76	339 5.3 ± 0.58	340 55.0 ± 1.19	341 20.0 ± 3.48
342 \neg (no-finetuning)	343 \checkmark	344 5.9 ± 0.84	345 35.2 ± 1.23	346 58.2 ± 1.23	347 24.0 ± 3.27
348 TaskCraft	349 \checkmark	350 14.6 ± 1.26	351 87.5 ± 0.85	352 64.3 ± 1.19	353 30.0 ± 3.72
354 MegaScience	355 \checkmark	356 14.2 ± 1.26	357 84.7 ± 0.93	358 62.3 ± 1.20	359 36.0 ± 3.90
360 MiroVerse	361 \checkmark	362 15.0 ± 1.28	363 84.5 ± 0.93	364 62.8 ± 1.20	365 32.0 ± 3.79
366 AgentFrontier	367 \checkmark	368 18.8 ± 1.32	369 86.8 ± 0.92	370 67.2 ± 1.18	371 40.0 ± 3.85
<i>372 Backbone: Qwen3-32B</i>					
373 \neg (no-finetuning)	374 \times	375 7.3 ± 0.98	376 5.8 ± 0.60	377 60.9 ± 1.15	378 37.0 ± 3.96
379 \neg (no-finetuning)	380 \checkmark	381 8.4 ± 0.92	382 48.6 ± 1.28	383 65.1 ± 1.18	384 39.0 ± 3.92
385 TaskCraft	386 \checkmark	387 18.4 ± 1.38	388 91.1 ± 0.73	389 66.2 ± 1.18	390 40.0 ± 3.98
391 MegaScience	392 \checkmark	393 18.5 ± 1.38	394 89.6 ± 0.78	395 68.4 ± 1.16	396 40.0 ± 3.98
397 MiroVerse	398 \checkmark	399 19.9 ± 1.42	400 87.7 ± 0.84	401 67.4 ± 1.16	402 43.0 ± 4.02
403 AgentFrontier	404 \checkmark	405 23.8 ± 1.52	406 90.9 ± 0.73	407 70.3 ± 1.14	408 51.0 ± 4.06
<i>409 Backbone: Qwen3-30B-A3B-Thinking-2507</i>					
410 \neg (no-finetuning)	411 \times	412 9.2 ± 1.06	413 4.9 ± 0.56	414 51.2 ± 1.07	415 32.0 ± 3.79
416 \neg (no-finetuning)	417 \checkmark	418 10.2 ± 1.08	419 47.2 ± 1.28	420 55.1 ± 1.13	421 40.0 ± 3.98
422 TaskCraft	423 \checkmark	424 19.9 ± 1.42	425 90.1 ± 0.76	426 72.3 ± 1.11	427 44.0 ± 4.08
428 MegaScience	429 \checkmark	430 20.2 ± 1.42	431 90.0 ± 0.77	432 73.1 ± 1.10	433 48.0 ± 4.08
434 MiroVerse	435 \checkmark	436 19.6 ± 1.42	437 86.7 ± 0.87	438 70.6 ± 1.13	439 49.0 ± 4.08
440 AgentFrontier	441 \checkmark	442 25.7 ± 1.50	443 91.4 ± 0.79	444 74.4 ± 1.13	445 54.0 ± 4.01

352 5 ANALYSIS

353 5.1 SENSITIVITY TO LKP / MKO CONFIGURATION

354 We conduct an ablation study on the Less Knowledgeable Peer (LKP) and More Knowledgeable
355 Other (MKO) configurations to assess our framework's sensitivity. The study investigates the trade-
356 off between **synthesis efficiency** (data yield) and **data complexity** (reasoning depth), aiming to
357 validate that our chosen configuration strikes an effective balance.

361 **Experimental Setup.** We evaluate three LKP/MKO configurations on a 1,000-sample subset of
362 D_{refined} to probe varying capability gaps. Note that DeepSeek-V3.1 possesses stronger reasoning and
363 agentic abilities than DeepSeek-R1 (Liu et al., 2024; Guo et al., 2025a). The configurations are: **(1)**
364 **Original (Balanced Gap)**, using DeepSeek-R1 (no tools) as LKP and DeepSeek-V3.1 (with tools)
365 as MKO; **(2) Wider Gap**, replacing the LKP with a weaker Qwen3-30B-A3B; and **(3) Narrower
366 Gap**, using DeepSeek-R1 for both roles, where the MKO is distinguished only by its access to tools.

367 **Results and Analysis.** As presented in Table 4, a **wider gap** (Config. 2) with a weaker LKP
368 increases the data yield by 44.1% but at the cost of complexity, evidenced by a sharp decrease in
369 average rounds ($\downarrow 44.3\%$) and tool calls ($\downarrow 63.4\%$). This results in simpler data, less effective for
370 advancing model capabilities. Conversely, a **narrower gap** (Config. 3), where models differ only
371 in tool access, maintains high complexity but suffers a 27.5% drop in yield, rendering it inefficient
372 for large-scale synthesis. These results empirically validate that our chosen **original configuration**
373 achieves a crucial trade-off, ensuring both scalable data generation and sufficient data complex-
374 ity. This demonstrates our model selection is a deliberate strategy to optimize this balance, not an
375 arbitrary choice.

378
 379 Table 3: Accuracy on the Humanity’s Last Exam (full text-only set). Results are reported across
 380 major knowledge domains. Each block corresponds to a different Qwen3 backbone. Numbers with
 381 a colored background denote the best within each block; underlined numbers denote the second best.

RFT Dataset	Tools	Domain Accuracy on Humanity’s Last Exam (%)								
		Math	CS/AI	Bio./Med.	Physics	Humanities	Chem.	Eng.	Other	Avg.
<i>Backbone: Qwen3-8B</i>										
– (no-finetuning)	✗	6.46	2.65	5.88	0.99	3.63	1.00	6.45	1.61	4.00
– (no-finetuning)	✓	6.26	3.54	9.05	2.48	7.25	7.00	6.45	5.14	5.94
TaskCraft	✓	16.21	<u>10.62</u>	14.93	<u>6.44</u>	<u>22.80</u>	9.00	9.68	15.43	14.58
MegaScience	✓	14.56	<u>10.62</u>	18.10	5.94	21.76	9.00	12.90	16.57	14.21
MiroVerse	✓	<u>17.33</u>	<u>10.62</u>	15.38	5.94	21.24	8.00	6.45	<u>17.71</u>	<u>15.00</u>
AgentFrontier	✓	22.46	14.16	<u>16.74</u>	10.40	24.35	11.00	6.45	19.43	18.80
<i>Backbone: Qwen3-32B</i>										
– (no-finetuning)	✗	8.72	5.75	10.41	0.50	7.77	8.00	6.45	5.14	7.34
– (no-finetuning)	✓	10.97	5.31	9.05	4.95	7.25	5.00	6.45	4.57	8.36
TaskCraft	✓	20.72	14.16	<u>16.74</u>	8.91	25.39	<u>14.00</u>	<u>14.52</u>	20.57	18.43
MegaScience	✓	21.23	<u>14.60</u>	14.93	6.44	29.02	12.00	11.29	<u>21.71</u>	18.52
MiroVerse	✓	<u>22.56</u>	14.16	<u>16.74</u>	<u>10.40</u>	34.72	12.00	6.45	20.57	<u>19.92</u>
AgentFrontier	✓	28.21	16.81	18.10	15.84	30.57	15.00	19.35	24.00	23.82
<i>Backbone: Qwen3-30B-A3B-Thinking-2507</i>										
– (no-finetuning)	✗	13.03	7.96	8.14	3.47	7.25	5.00	8.06	2.86	9.24
– (no-finetuning)	✓	13.13	7.96	6.33	1.98	11.92	10.00	6.45	10.29	10.17
TaskCraft	✓	24.62	12.39	16.29	7.92	21.76	<u>19.00</u>	12.90	22.29	19.87
MegaScience	✓	23.69	<u>14.60</u>	<u>20.81</u>	<u>9.90</u>	<u>26.94</u>	15.00	8.06	18.29	<u>20.15</u>
MiroVerse	✓	23.38	12.39	<u>20.81</u>	9.41	24.87	7.00	11.29	<u>22.86</u>	19.64
AgentFrontier	✓	29.85	16.81	21.27	17.82	31.61	22.00	14.52	28.00	25.67

402
 403 Table 4: Ablation study on LKP/MKO configurations, analyzing the trade-off between ZPD data
 404 yield and data complexity. The ZPD Data Yield is defined as the number of valid D_{ZPD} samples
 405 divided by the total candidate samples. Our original configuration (in bold) demonstrates a superior
 406 balance. S/Sc/B/C denotes Search, Scholar, Brower, and Code tools respectively.

Configuration (LKP / MKO)	ZPD Data Yield (%)	Avg. Rounds	Avg. Tool Calls	Tool Usage Dist. (S/Sc/B/C)
1. DS-R1 / DS-V3.1+T (Original)	33.1	3.32	2.32	0.32 / 0.66 / 0.82 / 0.52
2. Qwen3-30B / DS-V3.1+T (Wider Gap)	47.7 (<u>+44.1%</u>)	1.85 (<u>-44.3%</u>)	0.85 (<u>-63.4%</u>)	0.18 / 0.23 / 0.36 / 0.08 (all ↓)
3. DS-R1 / DS-R1+T (Narrower Gap)	24.0 (<u>-27.5%</u>)	2.99 (≈)	1.99 (≈)	0.19 / 0.67 / 0.58 / 0.55

5.2 BO(N) ANALYSIS: VALIDATING DIFFICULTY RICHNESS & POTENTIAL FOR RL TRAINING

415 To assess the difficulty distribution of AgentFrontier and
 416 the latent capabilities of the RFT model, we conducted a
 417 Best-of-N (BoN) analysis. On a held-out validation set of
 418 300 samples, we generated $N = 8$ independent solution
 419 trajectories for each task and measured the success rate if
 420 at least one of the N attempts was correct (pass@ N).

421 As shown in Figure 4, the accuracy dramatically increases
 422 from 21.7% at pass@1 to 40.7% at pass@8. This 19.0-
 423 point improvement provides two key insights. **First, it**
424 validates the designed difficulty of AgentFrontier: the
 425 dataset is not a binary mix of trivial and impossible tasks.
 426 Instead, it presents a challenging frontier where initial at-
 427 tempts may fail, but success is achievable through explo-
 428 ration. This provides a rich learning signal beyond superficial
 429 pattern matching. **Second, it highlights the significant potential for**
 430 **subsequent reinforcement learning (RL)** While supervised
 431 fine-tuning (SFT) trains the model on a single reference solution, the large gap between pass@1 and
 432 pass@8 confirms that for problems the model fails to solve on the first attempt, its policy distribution
 433 contains diverse and successful alternative trajectories. This is a crucial precondition for effective
 434 RL, ensuring that exploration can discover high-reward experiences necessary for effective policy

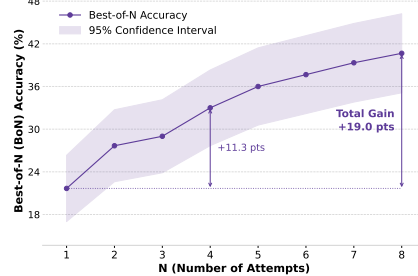


Figure 4: Best-of-N accuracy of our RFT Qwen3-30B-A3B on a 300-sample validation set from AgentFrontier.

optimization. Therefore, AgentFrontier serves not only as a robust training resources for SFT but also as a strong foundation for RL to further unlock an agent’s problem-solving potential.

5.3 WHY AGENTFRONTIER EXCELS: DISSECTING THE LEAP IN REASONING & TOOL-USE

From Shallow Retrieval to Deep Causal Reasoning. Figure 5 reveals the performance dynamics that underscore AgentFrontier’s superiority. The vast majority (95%) of problems are solved within a 15-round horizon, a critical window in which our RFT dataset consistently outperforms all fine-tuning dataset baselines. This advantage is a principled consequence of our data generation strategy rooted in the Zone of Proximal Development. By curating tasks that are unsolvable by the base model yet solvable with external scaffolding, we create training instances of optimal difficulty. This forces the model to abandon simplistic, single-source retrieval and instead master knowledge fusion—the non-trivial meta-skill of integrating disparate information streams into a coherent solution. The agent learns not merely what information to retrieve, but how to synthesize it, shifting from shallow pattern-matching to in-depth causal reasoning.

From High-Volume Invocation to High-Efficacy Orchestration. The design philosophy of AgentFrontier prioritizes the cultivation of strategic tool orchestrators over rote tool callers. Unlike datasets that promote skewed tool dependencies (e.g., code-centric MiroVerse or search-centric TaskCraft), AgentFrontier promotes a balanced tool-use distribution (Table 1). This forces the agent to develop a sophisticated understanding of inter-tool synergy rather than mastering a single tool in isolation. The results on the HLE benchmark (Table 5) confirm this empirical payoff. Our agent achieves a macro-average conditional tool accuracy of 26.3%—a significant leap from the 21% plateau of competitors—with a comparable number of interactions. This demonstrates that agent capability stems not from the volume of tool calls, but their efficacy. Our method trains the model to transition from high-volume, low-yield tool usage to precise, high-efficacy orchestration, which is a crucial step toward creating more resourceful agents.

Table 5: Tool usage statistics for the Qwen3-30B-A3B agent on the HLE text-only test set (2154 problems). Each column block shows performance after RFT on a different dataset. We report average usage per round and conditional tool accuracy (Acc, %), defined as the success rate for tasks that use the tool. The final row details overall metrics. Best results are in **bold**.

Tool / Metric	TaskCraft		MegaScience		MiroVerse		AgentFrontier	
	Usage	Acc (%)	Usage	Acc (%)	Usage	Acc (%)	Usage	Acc (%)
Search	0.68	19.6	0.67	20.3	0.73	20.4	0.73	24.9
Scholar	0.78	21.0	0.98	20.3	0.87	20.6	0.89	25.4
Browser	1.24	25.2	1.39	23.4	1.47	22.7	1.32	29.8
Code	0.52	18.1	0.65	18.6	0.67	18.4	0.63	24.9
Overall (Rounds/Acc.)	4.21	21.0	4.70	20.6	4.74	20.5	4.57	26.3

5.4 HOLISTIC AGENTIC TRAINING

Setup. We further investigate the benefits of a holistic training pipeline that incorporates continued pre-training (CPT) and post-training. Due to the large-scale GPU computation in CPT, this study is conducted only on Qwen3-30B-A3B-Thinking-2507 and our AgentFrontier data. The holistic training pipeline consists of two stages: (1) **Continued Pre-training (CPT)**: One epoch over 50B tokens, comprising 1 million summarized text chunks and 20 million knowledge-intensive QA pairs. (2) **Rejection Sampling Fine-tuning (RFT)**: Three epochs on 12,000 high-quality trajectories.

Evaluation. We conducted a comprehensive evaluation of our model, AgentFrontier-30B-A3B, against a broad spectrum of competitors: proprietary LLMs (OpenAI, 2024; anthropic, 2025; DeepMind, 2025) with tools, proprietary and prominent open-source deep-research agents (OpenAI, 2025a; Google, 2025; MoonshotAI, 2025; Wu et al., 2025; Li et al., 2025a; Tao et al., 2025).

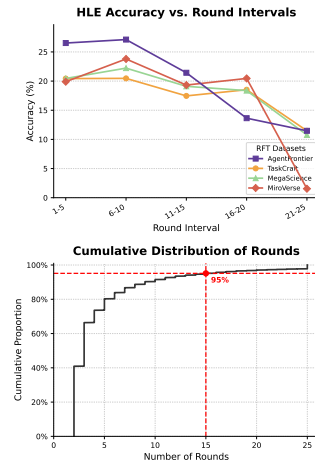


Figure 5: Accuracy vs. number of rounds on 4 datasets.

486
 487 **Results.** As shown in Table 6, our holisti-
 488 cally trained agent not only sets a new state-
 489 of-the-art among open-source models but also
 490 competes effectively with significantly larger,
 491 proprietary agents. The final row isolates the
 492 contribution of CPT, which consistently boosts
 493 performance across all benchmarks (+2.9 on
 494 HLE, +7.0 on xBench-ScienceQA). Notably,
 495 CPT yields a +2.0 point gain on ZPD Exam,
 496 where the RFT-only model’s performance was
 497 already near-saturation. This provides strong
 498 evidence that strengthening a model’s founda-
 499 tional knowledge via CPT directly enhances its
 500 capacity for complex agentic tasks.

501 5.5 CASE STUDY

502
 503 A qualitative analysis on an HLE case (Phan et al., 2025) (Appendix E) further illustrates our agent’s
 504 reasoning process. In a complex clinical scenario, OpenAI DeepResearch (OpenAI, 2025a) agent
 505 exhibited **diagnostic fixation**, misdiagnosing **Charcot Arthropathy** by focusing on common neg-
 506 ative findings like sterile synovial fluid. In contrast, our AgentFrontier agent correctly identified
 507 the key anomaly: the patient’s paradoxical worsening on prednisone. It hypothesized that this was
 508 due to a latent infection unmasked by immunosuppression, rather than an inflammatory rebound.
 509 This triggered a targeted inquiry, using a literature search to confirm that **Chronic Osteomyelitis** can
 510 present with sterile aspirates and is exacerbated by steroids. This progression from identifying an
 511 anomaly to forming a hypothesis and validating it with targeted research demonstrates AgentFront-
 512 ier’s advanced research capabilities.

513 514 6 RELATED WORK

515
 516 **Data Synthesis for LLM Agents.** Synthesizing high-quality data is critical for advancing LLM
 517 agents that require complex reasoning and tool use (Zeng et al., 2025; Liu et al., 2025; Zhou et al.,
 518 2024). Initial efforts replaced costly manual curation with programmatic generation, creating agentic
 519 tasks with verifiable solution trajectories (Shi et al., 2025; Hongjin et al., 2025; Huang et al., 2025).
 520 Subsequent research aimed to enhance data quality by grounding synthesis in external knowledge
 521 sources like scientific documents (Fan et al., 2025; Feng et al., 2025). While these approaches in-
 522 crease factual richness, they often produce tasks solvable via localized information retrieval, rather
 523 than promoting the deep knowledge integration essential for complex research (OpenAI, 2025a).
 524 A central challenge remains the precise calibration of task difficulty. Without a principled control
 525 mechanism, synthetic data risks being too simple for effective learning or too complex to yield a us-
 526 able training signal (Li et al., 2025b). These strategies rely on heuristics like incremental constraint
 527 addition (Patel et al., 2025) or probes to distinguish reasoning from recitation (Yan et al., 2025), yet
 528 lack a principled framework to calibrate difficulty for scaffolding complex reasoning.

530 531 7 CONCLUSION

532
 533 In this work, we presented a novel data synthesis paradigm based on the Zone of Proximal De-
 534 velopment (ZPD) theory. Our framework co-generates a targeted training resources and a self-
 535 evolving ZPD Exam to progressively enhance and evaluate agentic reasoning. The resulting model,
 536 AgentFrontier-30B-A3B, validates our approach by achieving state-of-the-art results on challenging
 537 expert-level multi-disciplinary benchmarks, surpassing even significantly larger proprietary agents.
 538 This work demonstrates that a principled, pedagogical approach to data synthesis is a highly effec-
 539 tive, if not essential, strategy for cultivating advanced reasoning abilities in a data-efficient manner.

Table 6: AgentFrontier-30B outperforms SOTA agents on four multi-disciplinary benchmarks. The performance gain from our CPT is shown in the final row. [†] marks results from official reports.

Agents	HLE	ZPD Exam	RBench-T	xBench-SciQA
<i>Proprietary LLMs with Tools & Deep-Research Agents</i>				
GPT-4o	4.8	51.3	48.5	15.0
Claude 4 Sonnet	14.3	86.6	71.1	47.0
Gemini 2.5 Flash	12.6	58.1	<u>75.8</u>	39.0
<i>Open-source Agents</i>				
WebDancer-QwQ-32B	6.4	51.8	67.6	38.0
WebSailor-72B	9.2	62.1	44.9	27.0
WebShaper-72B	8.0	54.4	66.8	29.0
<i>AgentFrontier-30B-A3B (Ours)</i>				
RFT only	25.7	<u>91.4</u>	74.4	<u>54.0</u>
CPT+RFT	28.6	93.4	77.1	61.0
Δ (CPT gain)	+2.9	+2.0	+2.7	+7.0

540 ETHICS STATEMENT
541542 All authors of this work have read and agree to adhere to the ICLR Code of Ethics. The corpora used
543 for data synthesis in our research are sourced from publicly available documents. We have ensured
544 that our use of this data complies with all applicable terms of use and licenses provided by the data
545 owners. The new training data generated through our pipeline will be made publicly available after
546 a thorough review to ensure its quality and safety.
547548 REPRODUCIBILITY STATEMENT
549550 We are committed to ensuring the full reproducibility of our research. All experimental scripts, full
551 training data and the trained weights of our AgentFrontier-30B-A3B model will be publicly released.
552553 For immediate verification during the review process, the paper and its supplementary materials
554 already include:
555

- **Evaluation Data:** The complete question-and-answer sets for all evaluation benchmarks used in our study.
- **Generated Examples:** A curated set of 100 question-and-answer examples from our AgentFrontier pipeline, provided for qualitative analysis.
- **Novel Benchmark:** The full ZPD Exam-v1 benchmark proposed in this work.
- **Implementation Details:** Detailed descriptions of training hyperparameters, tool implementation, and evaluation setup are available in Appendix C and D.
- **Prompts:** The exact prompts employed for our LLM-as-a-Judge, data filtering mechanisms and iterative agentic refinement are provided in Appendix F.

566 Together, these resources offer a transparent and direct pathway for verifying our findings and serve
567 as a foundation for future research.
568569 REFERENCES
570571 anthropic. Meet claude, 2025. URL <https://www.anthropic.com/claude>.
572573 Anthropic. Claude takes research to new places. <https://www.anthropic.com/news/research>, April 2025.
574576 Google DeepMind. Gemini 2.5, 2025. URL <https://blog.google/technology/google-deepmind/gemini-model-thinking-updates-march-2025/>.
577578 Xinrun Du, Yifan Yao, Kaijing Ma, Bingli Wang, Tianyu Zheng, King Zhu, Minghao Liu, Yiming Liang, Xiaolong Jin, Zhenlin Wei, et al. SuperGPQA: Scaling LLM evaluation across 285
579 graduate disciplines. *arXiv preprint arXiv:2502.14739*, 2025.
580582 Run-Ze Fan, Zengzhi Wang, and Pengfei Liu. Megascience: Pushing the frontiers of post-training
583 datasets for science reasoning. *arXiv preprint arXiv:2507.16812*, 2025.
584585 Yunzhen Feng, Elvis Dohmatob, Pu Yang, Francois Charton, and Julia Kempe. Beyond model
586 collapse: Scaling up with synthesized data requires verification. In *The Thirteenth International
587 Conference on Learning Representations*, 2025.588 Google. Deep research is now available on gemini 2.5 pro experimental., 2025. URL <https://blog.google/products/gemini/deep-research-gemini-2-5-pro-experimental/>.
589592 Daya Guo, Dejian Yang, Huawei Zhang, Junxiao Song, Ruoyu Zhang, Runxin Xu, Qihao Zhu,
593 Shirong Ma, Peiyi Wang, Xiao Bi, et al. DeepSeek-R1: Incentivizing reasoning capability in
LLMs via reinforcement learning. *arXiv preprint arXiv:2501.12948*, 2025a.
594

594 Meng-Hao Guo, Jiajun Xu, Yi Zhang, Jiaxi Song, Haoyang Peng, Yi-Xuan Deng, Xinzhi Dong, Kiy-
 595 ohiro Nakayama, Zhengyang Geng, Chen Wang, et al. Rbench: Graduate-level multi-disciplinary
 596 benchmarks for llm & mllm complex reasoning evaluation. In *Forty-second International Con-
 597 ference on Machine Learning*, 2025b.

598 Dan Hendrycks, Collin Burns, Steven Basart, Andy Zou, Mantas Mazeika, Dawn Song, and Jacob
 599 Steinhardt. Measuring massive multitask language understanding. In *ICLR*. OpenReview.net,
 600 2021.

602 SU Hongjin, Ruoxi Sun, Jinsung Yoon, Pengcheng Yin, Tao Yu, and Sercan O Arik. Learn-by-
 603 interact: A data-centric framework for self-adaptive agents in realistic environments. In *The
 604 Thirteenth International Conference on Learning Representations*, 2025.

605 Yue Huang, Siyuan Wu, Chujie Gao, Dongping Chen, Qihui Zhang, Yao Wan, Tianyi Zhou, Chaowei
 606 Xiao, Jianfeng Gao, Lichao Sun, et al. Datagen: Unified synthetic dataset generation via large
 607 language models. In *The Thirteenth International Conference on Learning Representations*, 2025.

609 Bowen Jin, Hansi Zeng, Zhenrui Yue, Jinsung Yoon, Sercan Arik, Dong Wang, Hamed Zamani, and
 610 Jiawei Han. Search-r1: Training llms to reason and leverage search engines with reinforcement
 611 learning. *arXiv preprint arXiv:2503.09516*, 2025.

612 Jina.ai. Jina, 2025. URL <https://jina.ai/>.

614 Patrick Lewis, Ethan Perez, Aleksandra Piktus, Fabio Petroni, Vladimir Karpukhin, Naman Goyal,
 615 Heinrich Kütller, Mike Lewis, Wen-tau Yih, Tim Rocktäschel, et al. Retrieval-augmented gener-
 616 ation for knowledge-intensive nlp tasks. *Advances in neural information processing systems*, 33:
 617 9459–9474, 2020.

619 Kuan Li, Zhongwang Zhang, Huirong Yin, Liwen Zhang, Litu Ou, Jialong Wu, Wenbiao Yin, Baix-
 620 uan Li, Zhengwei Tao, Xinyu Wang, et al. Websailor: Navigating super-human reasoning for web
 621 agent. *arXiv preprint arXiv:2507.02592*, 2025a.

622 Xiaochuan Li, Zichun Yu, and Chenyan Xiong. Montessori-instruct: Generate influential training
 623 data tailored for student learning. In *The Thirteenth International Conference on Learning Rep-
 624 resentations*, 2025b.

626 Xiaoxi Li, Guanting Dong, Jiajie Jin, Yuyao Zhang, Yujia Zhou, Yutao Zhu, Peitian Zhang, and
 627 Zhicheng Dou. Search-o1: Agentic search-enhanced large reasoning models. *arXiv preprint
 628 arXiv:2501.05366*, 2025c.

629 Xiaoxi Li, Jiajie Jin, Guanting Dong, Hongjin Qian, Yutao Zhu, Yongkang Wu, Ji-Rong Wen,
 630 and Zhicheng Dou. Webthinker: Empowering large reasoning models with deep research ca-
 631 pability. *CoRR*, abs/2504.21776, 2025d. doi: 10.48550/ARXIV.2504.21776. URL <https://doi.org/10.48550/arXiv.2504.21776>.

633 Aixin Liu, Bei Feng, Bing Xue, Bingxuan Wang, Bochao Wu, Chengda Lu, Chenggang Zhao,
 634 Chengqi Deng, Chenyu Zhang, Chong Ruan, et al. DeepSeek-V3 technical report. *arXiv preprint
 635 arXiv:2412.19437*, 2024.

637 Junteng Liu, Yuanxiang Fan, Zhuo Jiang, Han Ding, Yongyi Hu, Chi Zhang, Yiqi Shi, Shitong
 638 Weng, Aili Chen, Shiqi Chen, et al. Synlogic: Synthesizing verifiable reasoning data at scale for
 639 learning logical reasoning and beyond. *arXiv preprint arXiv:2505.19641*, 2025.

640 SA McLeod. Zone of proximal development, 2012.

642 Grégoire Mialon, Clémentine Fourrier, Thomas Wolf, Yann LeCun, and Thomas Scialom. Gaia:
 643 a benchmark for general ai assistants. In *The Twelfth International Conference on Learning
 644 Representations*, 2023.

646 MiroMind-Data-Team. Miroverse v0.1: A reproducible, full-trajectory, ever-growing deep re-
 647 search dataset, 2025. URL <https://huggingface.co/datasets/miromind-ai/MiroVerse-v0.1>.

648 MoonshotAI. Kimi-researcher, 2025. URL <https://moonshotai.github.io/Kimi-Researcher/>.

649

650

651 OpenAI. Hello GPT-4o, 2024. URL <https://openai.com/index/hello-gpt-4o/>.

652

653 OpenAI. Deep research system card, 2025a. URL <https://cdn.openai.com/deep-research-system-card.pdf>.

654

655 OpenAI. Introducing openai o3 and o4-mini, 2025b. URL <https://openai.com/index/introducing-o3-and-o4-mini/>.

656

657

658 Arkil Patel, Siva Reddy, and Dzmitry Bahdanau. How to get your llm to generate challenging

659 problems for evaluation. *arXiv preprint arXiv:2502.14678*, 2025.

660 Perplexity. Introducing perplexity deep research, 2025. URL <https://www.perplexity.ai/hub/blog/introducing-perplexity-deep-research>.

661

662

663 Long Phan, Alice Gatti, Ziwen Han, Nathaniel Li, Josephina Hu, Hugh Zhang, Chen Bo Calvin

664 Zhang, Mohamed Shaaban, John Ling, Sean Shi, et al. Humanity’s last exam. *arXiv preprint*

665 *arXiv:2501.14249*, 2025.

666 Zile Qiao, Guoxin Chen, Xuanzhong Chen, Donglei Yu, Wenbiao Yin, Xinyu Wang, Zhen Zhang,

667 Baixuan Li, Huifeng Yin, Kuan Li, et al. Webresearcher: Unleashing unbounded reasoning capa-

668 bility in long-horizon agents. *arXiv preprint arXiv:2509.13309*, 2025.

669

670 Yujia Qin, Shihao Liang, Yining Ye, Kunlun Zhu, Lan Yan, Yaxi Lu, Yankai Lin, Xin Cong, Xiangru

671 Tang, Bill Qian, Sihan Zhao, Lauren Hong, Runchu Tian, Ruobing Xie, Jie Zhou, Mark Gerstein,

672 dahai li, Zhiyuan Liu, and Maosong Sun. ToolLM: Facilitating large language models to master

673 16000+ real-world APIs. In *The Twelfth International Conference on Learning Representations*,

674 2024. URL <https://openreview.net/forum?id=dHng200Jjr>.

675

676 David Rein, Betty Li Hou, Asa Cooper Stickland, Jackson Petty, Richard Yuanzhe Pang, Julien

677 Dirani, Julian Michael, and Samuel R. Bowman. GPQA: A graduate-level Google-proof Q&A

678 benchmark. *CoRR*, abs/2311.12022, 2023.

679

680 Dingfeng Shi, Jingyi Cao, Qianben Chen, Weichen Sun, Weizhen Li, Hongxuan Lu, Fangchen Dong,

681 Tianrui Qin, King Zhu, Minghao Liu, et al. Taskcraft: Automated generation of agentic tasks.

682 *arXiv preprint arXiv:2506.10055*, 2025.

683

684 Noah Shinn, Federico Cassano, Ashwin Gopinath, Karthik Narasimhan, and Shunyu Yao. Reflexion:

685 Language agents with verbal reinforcement learning. *Advances in Neural Information Processing*

686 *Systems*, 36:8634–8652, 2023.

687

688 Mohammad Shoeybi, Mostafa Patwary, Raul Puri, Patrick LeGresley, Jared Casper, and Bryan

689 Catanzaro. Megatron-lm: Training multi-billion parameter language models using model par-

690 allelism. *arXiv preprint arXiv:1909.08053*, 2019.

691

692 Dan Su, Kezhi Kong, Ying Lin, Joseph Jennings, Brandon Norick, Markus Kliegl, Mostafa Patwary,

693 Mohammad Shoeybi, and Bryan Catanzaro. Nemotron-CC: Transforming Common Crawl into a

694 refined long-horizon pretraining dataset. In Wanxiang Che, Joyce Nabende, Ekaterina Shutova,

695 and Mohammad Taher Pilehvar (eds.), *Proceedings of the 63rd Annual Meeting of the Association*

696 *for Computational Linguistics (Volume 1: Long Papers)*, pp. 2459–2475, Vienna, Austria, July

697 2025. Association for Computational Linguistics. ISBN 979-8-89176-251-0. doi: 10.18653/v1/

698 2025.acl-long.123. URL <https://aclanthology.org/2025.acl-long.123/>.

699

700 Zhengwei Tao, Jialong Wu, Wenbiao Yin, Junkai Zhang, Baixuan Li, Haiyang Shen, Kuan Li,

701 Liwen Zhang, Xinyu Wang, Yong Jiang, et al. Webshaper: Agentically data synthesizing via

702 information-seeking formalization. *arXiv preprint arXiv:2507.15061*, 2025.

703

704 Minyang Tian, Luyu Gao, Shizhuo Zhang, Xianan Chen, Cunwei Fan, Xuefei Guo, Roland Haas,

705 Pan Ji, Kittithat Krongchon, Yao Li, et al. Scicode: A research coding benchmark curated by

706 scientists. *Advances in Neural Information Processing Systems*, 37:30624–30650, 2024.

702 Lev S Vygotsky. *Mind in society: The development of higher psychological processes*, volume 86.
 703 Harvard university press, 1978.
 704

705 Fanqi Wan, Xinting Huang, Deng Cai, Xiaojun Quan, Wei Bi, and Shuming Shi. Knowledge fusion
 706 of large language models. In *The Twelfth International Conference on Learning Representations*,
 707 2024. URL <https://openreview.net/forum?id=jiDs12qcz>.

708 Yubo Wang, Xueguang Ma, Ge Zhang, Yuansheng Ni, Abhranil Chandra, Shiguang Guo, Weiming
 709 Ren, Aaran Arulraj, Xuan He, Ziyan Jiang, Tianle Li, Max Ku, Kai Wang, Alex Zhuang, Rongqi
 710 Fan, Xiang Yue, and Wenhui Chen. MMLU-Pro: A more robust and challenging multi-task lan-
 711 guage understanding benchmark. *CoRR*, abs/2406.01574, 2024.

712 Jason Wei, Zhiqing Sun, Spencer Papay, Scott McKinney, Jeffrey Han, Isa Fulford, Hyung Won
 713 Chung, Alex Tachard Passos, William Fedus, and Amelia Glaese. Browsecmp: A simple yet
 714 challenging benchmark for browsing agents. *arXiv preprint arXiv:2504.12516*, 2025.
 715

716 Jialong Wu, Baixuan Li, Runnan Fang, Wenbiao Yin, Liwen Zhang, Zhengwei Tao, Dingchu Zhang,
 717 Zekun Xi, Yong Jiang, Pengjun Xie, et al. Webdancer: Towards autonomous information seeking
 718 agency. *arXiv preprint arXiv:2505.22648*, 2025.

719 xAI. Grok 3 beta — the age of reasoning agents, 2025. URL <https://x.ai/news/grok-3>.
 720

721 Xbench-Team. Xbench-deepsearch, 2025. URL <https://xbench.org/agi/aisearch>.
 722

723 Kai Yan, Yufei Xu, Zhengyin Du, Xuesong Yao, Zheyu Wang, Xiaowen Guo, and Jiecao Chen.
 724 Recitation over reasoning: How cutting-edge language models can fail on elementary school-
 725 level reasoning problems? *arXiv preprint arXiv:2504.00509*, 2025.

726 An Yang, Anfeng Li, Baosong Yang, Beichen Zhang, Binyuan Hui, Bo Zheng, Bowen Yu,
 727 Chang Gao, Chengan Huang, Chenxu Lv, et al. Qwen3 technical report. *arXiv preprint
 728 arXiv:2505.09388*, 2025.

729 Shunyu Yao, Jeffrey Zhao, Dian Yu, Nan Du, Izhak Shafran, Karthik Narasimhan, and Yuan Cao.
 730 React: Synergizing reasoning and acting in language models. In *International Conference on
 731 Learning Representations (ICLR)*, 2023.
 732

733 Weizhe Yuan, Jane Yu, Song Jiang, Karthik Padthe, Yang Li, Ilia Kulikov, Kyunghyun Cho, Dong
 734 Wang, Yuandong Tian, Jason E Weston, et al. Naturalreasoning: Reasoning in the wild with 2.8
 735 m challenging questions. *arXiv preprint arXiv:2502.13124*, 2025.

736 Aohan Zeng, Xin Lv, Qinkai Zheng, Zhenyu Hou, Bin Chen, Chengxing Xie, Cunxiang Wang,
 737 Da Yin, Hao Zeng, Jiajie Zhang, et al. Glm-4.5: Agentic, reasoning, and coding (arc) foundation
 738 models. *arXiv preprint arXiv:2508.06471*, 2025.

739 Yanzhao Zhang, Mingxin Li, Dingkun Long, Xin Zhang, Huan Lin, Baosong Yang, Pengjun Xie,
 740 An Yang, Dayiheng Liu, Junyang Lin, Fei Huang, and Jingren Zhou. Qwen3 embedding: Advanc-
 741 ing text embedding and reranking through foundation models. *arXiv preprint arXiv:2506.05176*,
 742 2025.
 743

744 Kun Zhou, Beichen Zhang, Zhipeng Chen, Xin Zhao, Jing Sha, Zhichao Sheng, Shijin Wang, Ji-
 745 Rong Wen, et al. Jiuzhang3. 0: Efficiently improving mathematical reasoning by training small
 746 data synthesis models. *Advances in Neural Information Processing Systems*, 37:1854–1889, 2024.
 747

748

749 APPENDIX

750 A THE USE OF LARGE LANGUAGE MODELS (LLMs)

751 During the preparation of this manuscript, we utilized Large Language Models (LLMs) for assis-
 752 tance with language proofreading (including grammar, spelling, and word choice) and for generating
 753 L^AT_EX code for tables and figures. The core intellectual contributions, including research ideation,
 754 analysis, and the substantive writing, are entirely the work of the authors.
 755

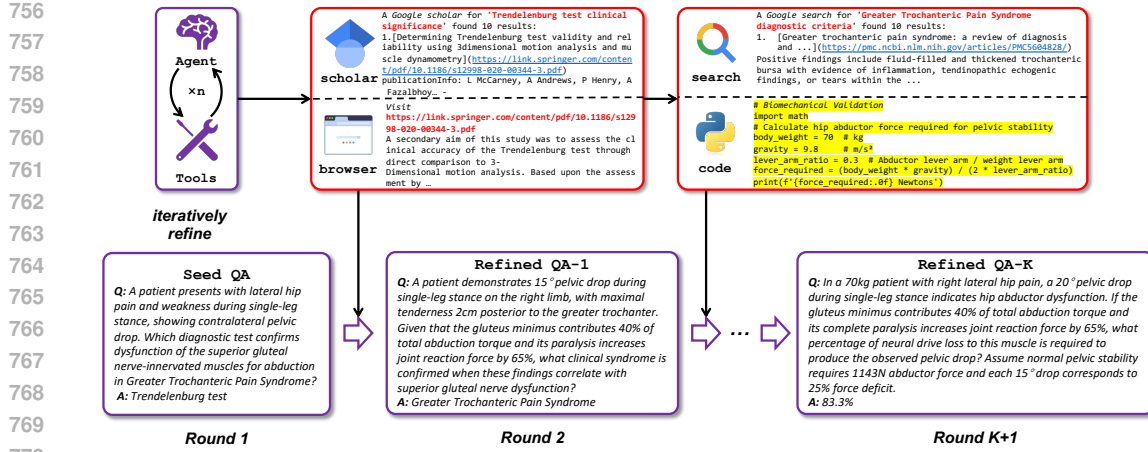


Figure 6: An overview of our iterative refinement process. We start with a biomedical seed QA, which is then refined into a complex diagnostic reasoning problem by synthesizing knowledge from academic literature. Finally, this problem is evolved into a practical computational challenge grounded in a real-world application, a process involving web search and programmatic validation.

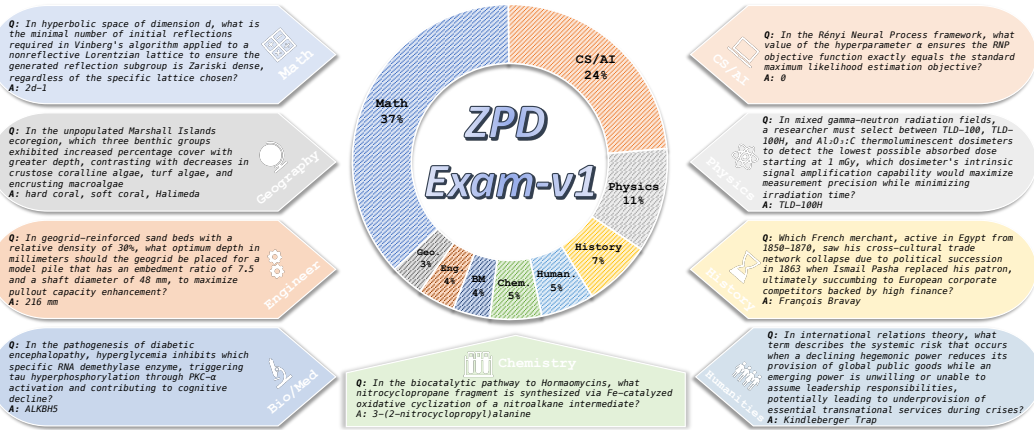


Figure 7: The ZPD Exam-v1 consists of 1024 questions categorized into 9 disciplines: Mathematics, Computer Science / Artificial Intelligence, Physics, History, Humanities, Chemistry, Biology / Medicine, Engineering, and Geography.

B MORE RELATED WORK

Multi-disciplinary Benchmark. The evaluation of advanced reasoning in large language models (LLMs) was pioneered by MMLU (Hendrycks et al., 2021), which set the standard for assessing multi-disciplinary knowledge. This led to a wave of subsequent benchmarks (Rein et al., 2023; Wang et al., 2024; Du et al., 2025; Guo et al., 2025b; Xbench-Team, 2025) targeting undergraduate or graduate level knowledge. However, the rapid progress of frontier models (OpenAI, 2025b; DeepMind, 2025; anthropic, 2025) is causing performance saturation on these static benchmarks, reducing their effectiveness in differentiating top-tier models. While newer benchmarks like Humanity’s Last Exam (Phan et al., 2025) increase difficulty through expert curation, they remain fixed assessments. In contrast, our work introduces the ZPD Exam, a self-evolving evaluation framework that adapts in lockstep with model capabilities, providing a consistently challenging frontier for LLM agent evaluation.

Deep-Research Agents. Deep-research agent, a system built upon large reasoning models (LRMs), is designed to automate multi-step search and reasoning. It empowers users to complete complex, cross-domain information synthesis and in-depth research tasks in minutes, a process that would oth-

erwise require hours of human effort. Proprietary agents (OpenAI, 2025a; Google, 2025; Anthropic, 2025; xAI, 2025; Perplexity, 2025; MoonshotAI, 2025) have demonstrated impressive capabilities in complex, multi-step research tasks. The open-source community has fostered a rich ecosystem of transparent and reproducible agents (Jin et al., 2025; Li et al., 2025c,d; Tao et al., 2025; Li et al., 2025a; Qiao et al., 2025). These efforts typically leverage explicit planning, tool-use, and web navigation to emulate human research processes, advancing the field through shared methodologies.

C DATA ENGINE DETAILS

This section provides a detailed breakdown of the hyperparameters, procedural logic, and computational costs associated with the AgentFrontier Data Engine, as outlined in Algorithm 1. These details are provided to ensure the transparency and reproducibility of our data synthesis framework.

C.1 HYPERPARAMETER CONFIGURATION

The data generation pipeline is governed by several key hyperparameters that control the granularity of data sourcing, the complexity of generated questions, and the strictness of the filtering process. Our configuration is as follows:

- **Thematic Coherence Threshold (τ_{theme}):** Set to **0.8**. This value determines the minimum semantic similarity required between text chunks to form a "composite unit" for seed question generation. A higher value ensures that initial questions are synthesized from thematically tighter content, promoting knowledge fusion.
- **Nearest Neighbors for Seeding (k_{nn}):** Set to **10**. During seed generation, for each text chunk, we retrieve its k_{nn} nearest neighbors to search for coherent triplets. This balances computational efficiency with a sufficiently large search space for discovering novel combinations.
- **Maximum Refinement Iterations (K_{max}):** Set to **30**. This parameter defines the maximum number of complexity escalation steps for any given QA pair in Stage II. This upper bound prevents infinite loops and manages computational resources.
- **Best-of-N (BoN) Verification Size (N):** Set to **3**. In the ZPD-filtering stage, the More Knowledgeable Other (\mathcal{A}_{MKO}) makes N independent attempts to solve a problem. This helps to reduce the variance in the agent's performance and provides a more reliable signal of whether a task is solvable.
- **Diversity Filter Threshold (ϵ):** Set to **0.7**. To ensure dataset diversity, a new QA pair is discarded if its question's semantic similarity to any existing question in \mathcal{D}_{ZPD} exceeds this threshold. The similarity is measured by a state-of-the-art reranker model.

C.2 AGENTIC REFINEMENT AND STOPPING CRITERION

The core of our data engine is the iterative refinement loop (Stage II), driven by the agent $\mathcal{A}_{\text{refine}}$. The goal of the escalation operator, Ψ_{escalate} , is to progressively increase the cognitive load required to answer a question. This is achieved by prompting the agent to perform a series of enrichment actions, including but not limited to: expanding the question with new, relevant concepts discovered through tool use; abstracting a general principle from specific examples; grounding the problem in a more complex, realistic context; or transforming a qualitative problem into a quantitative one requiring computation.

The iterative escalation is guided by a principled stopping criterion tied to the ZPD framework: for a given QA pair, the refinement loop terminates when the generated question q_k becomes unsolvable by the **Less Knowledgeable Peer** (\mathcal{A}_{LKP}), a baseline model formally defined in Stage III, or when a predefined maximum of $K_{\text{max}} = 30$ iterations is reached. This targeted termination ensures that the engine's computational resources are focused on producing problems that precisely challenge the base model's capabilities. In our experiments, the \mathcal{A}_{LKP} is instantiated as DeepSeek-R1-0528 without tool access.

864

Algorithm 1 AgentFrontier Data Engine Pipeline

865

866

867

868

869

870

871

872

873

874

875

876

877

878

879

880

881

882

883

884

885

886

887

888

889

890

891

892

893

894

895

896

897

898

899

900

901

902

903

904

905

906

907

908

909

910

911

912

913

914

915

916

917

Input: \mathcal{C}_{raw} : Raw document corpus Φ_{chunk} : Chunking model $\mathcal{M}_{\text{gen}}, \mathcal{A}_{\text{refine}}, \mathcal{A}_{\text{LKP}}, \mathcal{A}_{\text{MKO}}$: Models and agents

Sim, IsCorrect, IsSolvableBy: Similarity and evaluation functions

 $\tau_{\text{theme}}, K, N, \epsilon, k_{\text{nn}}$: Hyperparameters (thematic threshold, escalation steps, BoN size, redundancy threshold, number of neighbors)**Output:** \mathcal{D}_{ZPD} : Calibrated training dataset for post-training $\mathcal{D}_{\text{pretrain}}$: Dataset for continued pre-training $\mathcal{D}_{\text{human}}$: Dataset for human review1: **procedure** GENERATEZPDDATA($\mathcal{C}_{\text{raw}}, \dots$)2: $\mathcal{D}_{\text{ZPD}}, \mathcal{D}_{\text{pretrain}}, \mathcal{D}_{\text{human}} \leftarrow \emptyset, \emptyset, \emptyset$ **Stage I: Seed Question Generation**

▷ Preprocess corpus into semantic chunks

3: $\mathcal{C}_{\text{chunk}} \leftarrow \bigcup_{d \in \mathcal{C}_{\text{raw}}} \Phi_{\text{chunk}}(d)$ 4: $\mathcal{V}_{\text{index}} \leftarrow \text{BuildVectorIndex}(\mathcal{C}_{\text{chunk}})$ 5: $\mathcal{D}_{\text{seed}} \leftarrow \emptyset$ 6: **for** each chunk $c_i \in \mathcal{C}_{\text{chunk}}$ **do**7: $\mathcal{N}_i \leftarrow \text{FindNearestNeighbors}(c_i, \mathcal{V}_{\text{index}}, k_{\text{nn}})$ ▷ Find k-NN for efficient combination8: **for** each pair (c_j, c_k) from \mathcal{N}_i **do**9: **if** $\text{Sim}(c_i, c_j) > \tau_{\text{theme}} \wedge \text{Sim}(c_i, c_k) > \tau_{\text{theme}} \wedge \text{Sim}(c_j, c_k) > \tau_{\text{theme}}$ **then**10: $(q_0, a_0) \leftarrow \mathcal{M}_{\text{gen}}(\{c_i, c_j, c_k\})$ ▷ Generate QA from thematic unit11: $\mathcal{D}_{\text{seed}} \leftarrow \mathcal{D}_{\text{seed}} \cup \{(q_0, a_0)\}$ 12: **end if**13: **end for**14: **end for****Stages II & III: Iterative Escalation and ZPD Calibration**

▷ Initialize index for ZPD-set diversity check

15: $\mathcal{V}_{\text{ZPD}} \leftarrow \text{BuildVectorIndex}(\emptyset)$ 16: **for** each (q_0, a_0) in $\mathcal{D}_{\text{seed}}$ **do**17: $(q, a) \leftarrow (q_0, a_0)$ **Stage II: Agentic Refinement**

▷ Iteratively escalate complexity

18: **for** $k = 1$ to K **do**19: $(q, a) \leftarrow \Psi_{\text{escalate}}(q, a, \mathcal{A}_{\text{refine}})$ ▷ e.g., Expand, Abstract, Ground, etc.20: **end for****Stage III: ZPD-based Filtering**

▷ Check if too easy for Less Knowledgeable Peer

21: **if** $\text{IsSolvableBy}(\mathcal{A}_{\text{LKP}}, q, a)$ **then**22: $\mathcal{D}_{\text{pretrain}} \leftarrow \mathcal{D}_{\text{pretrain}} \cup \{(q, a)\}$ 23: **else**

▷ Challenging for LKP, now verify with MKO

24: $S_{\text{solutions}} \leftarrow \{\mathcal{A}_{\text{MKO}}(q) \text{ for } i = 1 \dots N\}$ ▷ Best-of-N by More Knowledgeable Other25: **if** $\exists s \in S_{\text{solutions}}$ s.t. $\text{IsCorrect}(s, a)$ **then** ▷ Verified as solvable, thus within ZPD26: $q_{\text{nearest}} \leftarrow \text{FindNearestNeighbor}(q, \mathcal{V}_{\text{ZPD}})$ 27: **if** $q_{\text{nearest}} = \emptyset$ or $\text{Sim}(q, q_{\text{nearest}}) < \epsilon$ **then**

▷ Filter for diversity

28: $\mathcal{D}_{\text{ZPD}} \leftarrow \mathcal{D}_{\text{ZPD}} \cup \{(q, a)\}$ 29: $\text{UpdateVectorIndex}(\mathcal{V}_{\text{ZPD}}, q)$ 30: **end if**

31: ▷ Unsolvable by MKO, potentially flawed or too hard

32: $\mathcal{D}_{\text{human}} \leftarrow \mathcal{D}_{\text{human}} \cup \{(q, a)\}$ 33: **end if**34: **end if**35: **end for**36: **return** $\mathcal{D}_{\text{ZPD}}, \mathcal{D}_{\text{pretrain}}, \mathcal{D}_{\text{human}}$ 37: **end procedure**

918 C.3 COMPUTATIONAL COST ANALYSIS
919920 We provide a detailed analysis of the computational cost required to generate a single high-quality
921 data point for the \mathcal{D}_{ZPD} dataset. The cost is broken down into the two primary stages of our pipeline:
922 agentic refinement and MKO verification. All token counts are based on the respective model's
923 tokenizer, and costs are estimated using official API pricing as of the experiment date¹.
924925 C.3.1 COST OF AGENTIC REFINEMENT (STAGE II)
926927 In this stage, the refinement agent, $\mathcal{A}_{\text{refine}}$ (DeepSeek-R1), iteratively enhances a QA pair until it
928 reaches the capability frontier of the Less Knowledge Peer (LKP). The cost per data point is variable,
929 depending on the number of iterations (K) needed.
930931 On average, processing a single candidate data point involves the following:
932933

- **Refinement Iterations (K):** A data point undergoes an average of **7.81** iterations.
- **Token Throughput per API Call:**
 - Input: **18,613.82** tokens.
 - Output: **11,643.22** tokens.
- **Tool Calls per Data Point:**
 - Search: **0.70** calls.
 - Scholar: **0.61** calls.
 - Browser: **1.21** calls (avg. 10,000 tokens/call).
 - Code Interpreter: **0.94** calls (executed locally, no API cost).

937 **Cost Breakdown.** The average refinement cost per candidate is approximately **\$0.24**, calculated
938 as follows:
939940

- **LLM Cost:** $7.81 \times (18,614 \times \$0.56/M + 11,643 \times \$1.68/M) \approx \0.234 .
- **Search Cost:** $(0.70 + 0.61) \times \$0.00275/\text{call} \approx \0.0036 .
- **Browser Cost:** $1.21 \times 10,000 \times \$0.00005/\text{token} \approx \0.0006 .

941 C.3.2 COST OF MKO VERIFICATION (STAGE III)
942943 Candidates that pass the refinement stage are then verified by the More Knowledgeable Other agent,
944 \mathcal{A}_{MKO} (DeepSeek-V3.1 with tools). This Best-of-N ($N = 3$) verification confirms that the prob-
945 lem is solvable by an expert-level agent, thus ensuring its placement within the Zone of Proximal
946 Development (ZPD).
947948 For the $N = 3$ verification attempts on a single candidate, the average resource consumption is:
949950

- **Total API Calls:** **3.32** calls.
- **Token Throughput per API Call:**
 - Input: **20,181.57** tokens.
 - Output: **24,169.88** tokens.
- **Total Tool Calls:**
 - Search: **0.50** calls.
 - Scholar: **0.92** calls.
 - Browser: **1.30** calls (avg. 10,000 tokens/call).
 - Code Interpreter: **0.53** calls (executed locally, no API cost).

951 ¹Pricing references: DeepSeek Model API (<https://api-docs.deepseek.com/>), SerpApi for
952 Google Search (<https://serpapi.com/enterprise>), and Jina Reader API (<https://jina.ai/>
953 reader/)

972 **Cost Breakdown.** The verification cost for a single candidate is approximately **\$0.18**:
 973

974 • **LLM Cost:** $3.32 \times (20,182 \times \$0.56/M + 24,170 \times \$1.68/M) \approx \0.172 .
 975 • **Search Cost:** $(0.50 + 0.92) \times \$0.00275/\text{call} \approx \0.0039 .
 976 • **Browser Cost:** $1.30 \times 10,000 \times \$0.00005/\text{token} \approx \0.00065 .
 977

978 However, only a fraction of candidates pass this stage. With an observed success rate of **33%**, the
 979 amortized cost to obtain one successfully verified data point is $\$0.18/0.33 \approx \0.54 .
 980

981 In summary, the total end-to-end amortized cost to generate one high-quality, verified PhD-level QA
 982 pair with its solution trajectory for \mathcal{D}_{ZPD} is approximately **\$0.78** ($\0.24 for refinement + $\$0.54$ for
 983 amortized verification). While this represents a non-trivial investment per sample, it aligns with our
 984 "quality-over-quantity" approach. This automated pipeline produces a valuable training asset at a
 985 fraction of the cost and time that manual curation by human experts would demand.

986 **C.4 HUMAN EVALUATION OF DATASET QUALITY**
 987

988 **C.4.1 HUMAN REVIEW FOR $\mathcal{D}_{\text{HUMAN}}$**
 989

990 We emphasize that $\mathcal{D}_{\text{human}}$ set is not used for any training. It serves as a diagnostic dataset, composed
 991 of samples that our most capable agent (the MKO) failed to solve. The purpose of $\mathcal{D}_{\text{human}}$ is to
 992 facilitate in-depth failure analysis, enabling us to understand the limitations of our synthesis engine
 993 and to probe the capability frontiers of state-of-the-art (SOTA) agents.

994 We conduct a qualitative audit on $\mathcal{D}_{\text{human}}$ set by randomly selecting 200 samples from $\mathcal{D}_{\text{human}}$ for
 995 manual inspection. For each discipline (e.g., CS, Math, and Biology), the review was performed
 996 by three graduate students with relevant expertise. Their task was to diagnose the root cause of the
 997 MKO's failure and classify each case into one of three predefined categories:
 998

999 (A) **Problem Defect:** The problem statement or its ground-truth answer is flawed (e.g., am-
 1000 biguous, ill-posed, or factually incorrect).
 1001 (B) **Execution Gap:** The agent devised a correct high-level plan but failed in its execution
 1002 (e.g., misinterpreting a retrieved source, overlooking contradictory evidence, or failing to
 1003 self-correct).
 1004 (C) **Strategic Planning Failure:** The agent failed to formulate a viable high-level plan to solve
 1005 the problem.
 1006

1007 Our analysis, summarized in Table 7, reveals that the vast majority of failures stem from agent's
 1008 intrinsic limitations rather than from data quality issues.
 1009

1010 **Table 7: Distribution of Failure Modes in $\mathcal{D}_{\text{human}}$**
 1011

Failure Type	Percentage (%)
(A) Problem Defect	10.5
(B) Execution Gap	71.0
(C) Strategic Planning Failure	18.5

1017 The predominance of "Execution Gap"(71.0%) is particularly informative. It reveals that even when
 1018 the MKO can devise a correct strategy, it often fails at the last mile of reasoning. The following case
 1019 study, involving a specialized structural biology question, illustrates this phenomenon:
 1020

1021 **Case Study: An Execution Gap in Structural Biology**
 1022

1023 **Question:** What minimum interatomic spacing must exist between the C γ 2 methyl groups
 1024 of β -branched residues at position d in coiled-coil hydrophobic cores to prevent steric
 1025 clashes?
 1026

1027 **Agent's Reasoning Trajectory:**
 1028

1026
1027
1028
1029
1030
1031
1032
1033
1034
1035
1036
1037
1038
1039
1040
1041
1042
1043
1044
1045
1046
1047
1048
1049
1050
1051
1052
1053
1054
1055
1056
1057
1058
1059
1060
1061
1062
1063
1064
1065
1066
1067
1068
1069
1070
1071
1072
1073
1074
1075
1076
1077
1078
1079

1. **Correct Initial Strategy:** The agent correctly initiated its research using `google scholar` and identified a highly relevant paper (Ramos and Lazaridis, 2011).
`google scholar(query="...")`
2. **Successful Information Extraction:** It subsequently employed the `Visit` tool on the paper’s PDF, correctly extracting the key quantitative detail: a distance range of 3.6–3.8 Å for valine. `Visit(url="...")`
3. **Failure in Final Synthesis:** Despite possessing the correct information, the agent prematurely concluded its reasoning. It presented 3.6 Å as the final answer, failing to perform a crucial validation step. Specifically, it did not reconcile this value with the ground truth (>5.5 Å), a discrepancy that could have been resolved by considering a different biological context discussed elsewhere in the same paper.

Analysis: This case is a clear example of an Execution Gap. The failure was not strategic but tactical, stemming from a lack of critical self-assessment and an over-reliance on the first piece of retrieved information. This underscores the need to advance agent capabilities beyond mere information retrieval towards robust and critical synthesis of retrieved knowledge.

This human-in-the-loop analysis establishes an invaluable feedback loop for our research:

1. **Data Quality Refinement:** It enables us to identify and filter the small fraction of flawed problems (Category A), thereby continuously enhancing the quality of our data synthesis engine in future iterations.
2. **Agent Capability Diagnosis:** More importantly, it provides a detailed qualitative map of the MKO’s reasoning deficiencies (Category B) and confirms that our synthesis engine generates data that genuinely challenge the capabilities of SOTA agents (Category C).

C.4.2 HUMAN REVIEW FOR \mathcal{D}_{ZPD}

Ensuring the quality of a fully synthetic dataset is paramount. In addition to flagging unsolvable cases for review, we conducted a rigorous quality control on the final training set. We randomly sampled 200 verified QA pairs from \mathcal{D}_{ZPD} for manual inspection by graduate students with domain expertise. The audit protocol required them to assess each sample against two strict criteria:

- **Problem Quality:** The question must be well-posed, non-trivial, and demonstrably at a postgraduate level of difficulty.
- **Solution Quality:** The agent-generated solution trajectory must be factually correct, logically sound, and exhibit a coherent and valid reasoning process.

The results were highly positive: over 96.5% of the audited samples passed this inspection, confirming the efficacy of our ZPD-based data generation and filtering pipeline.

C.5 A QUANTITATIVE ANALYSIS OF TASK DIFFICULTY

To provide direct evidence of the diverse cognitive challenges embedded in `AgentFrontier`, we performed a manual analysis to classify the nature of difficulty in our generated tasks. We annotated a random sample of 200 questions from the dataset, categorizing each according to its primary source of difficulty. This process yielded a robust distribution of cognitive demands, as detailed in Table 8.

The results in Table 8 clearly demonstrate that no single difficulty type dominates the dataset. The prevalence of **Quantitative Reasoning** (39.0%) and **Knowledge Fusion** (27.0%) substantiates our claim that `AgentFrontier` moves far beyond tasks solvable by simple information retrieval or linear tool chaining. Instead, it generates complex, realistic research challenges that compel agents to perform multi-faceted reasoning, such as executing code and integrating knowledge across diverse domains.

In summary, this quantitative analysis, combined with our principled multi-faceted design (Section 2) and the empirical evidence from diverse tool usage (Section 5.2), converges to demonstrate that `AgentFrontier` successfully fosters a rich and realistic spectrum of difficulty.

1080 Table 8: Distribution of primary difficulty types in a random sample of 200 AgentFrontier
 1081 questions. The analysis reveals a balanced composition, with a significant emphasis on reasoning-
 1082 intensive categories over simple retrieval.

Difficulty Type	Description	Percentage (%)
Knowledge Fusion	Requires synthesizing information from multiple, often interdisciplinary, sources to form a coherent conclusion.	27.0
Quantitative Reasoning	Demands mathematical calculation, logical deduction, or programmatic execution to arrive at a solution.	39.0
Conceptual Leap	Involves abstracting general principles or theories from concrete examples or identifying non-obvious relationships.	16.5
Critical Thinking	Necessitates identifying contradictions, evaluating the quality of evidence, or reasoning about anomalies and edge cases.	17.5

D EXPERIMENTAL DETAILS

D.1 EVALUATION BENCHMARKS

- **HLE** (Phan et al., 2025) - Humanity’s Last Exam is an expert-curated benchmark comprising 2,500 challenging questions across a wide range of disciplines, designed to assess frontier-level academic competence. Our evaluation is conducted on its 2,154 text-only questions.
- **ZPD Exam** - Our newly proposed multi-disciplinary benchmark designed to probe the zone of proximal development (ZPD) in LLMs. We use the 1,024 questions from its first version (v1.0).
- **R-Bench** (Guo et al., 2025b) - A graduate-level, multi-disciplinary benchmark designed to assess the complex reasoning capabilities of LLMs. We use its English text-only version. After excluding one question due to potential ambiguity, our evaluation set consists of 1,093 multiple-choice questions.
- **xBench-ScienceQA** (Xbench-Team, 2025) - A curated set of 100 Chinese question-answering items from the xBench suite, designed to evaluate foundational scientific knowledge.

D.2 BASELINE FINE-TUNING DATASETS

- **TaskCraft** (Shi et al., 2025) - The TaskCraft dataset facilitates the fine-tuning of agent models by programmatically generating agentic tasks at scale. These tasks are characterized by their inclusion of multiple tools, tiered difficulty levels, and verifiable execution trajectories.
- **MegaScience** (Fan et al., 2025) - The MegaScience dataset is constructed by integrating high-quality subsets from multiple open-source scientific datasets to ensure sample abundance and high fidelity. The majority of its questions are sourced from university textbooks.
- **MiroVerse** (MiroMind-Data-Team, 2025) - MiroVerse is an open-source, large-scale dataset for AI agents, covering diverse tasks such as multi-hop question answering, web navigation, and scientific reasoning. We use the SFT data from its v0.1 release.

D.3 TOOL IMPLEMENTATION

1132 Our agent is equipped with a suite of tools to support its research process, from broad exploration to
 1133 empirical validation. Each tool is designed for batch processing to enhance efficiency and produces
 structured outputs for seamless integration into the agent’s iterative reasoning loop.

- **Search:** Performs parallel web searches using the Google Search API. It returns a list of structured results, each containing a title, snippet, and URL, allowing the agent to efficiently assess the relevance of multiple sources.
- **Scholar:** Tackles multi-disciplinary challenges by querying the Google Scholar API to navigate scientific literature. It returns structured metadata, including authors, publication venue, and citation counts, enabling the agent to identify authoritative works and their scholarly context.
- **Browser:** Extracts targeted information from a given URL. The agent provides a specific goal (e.g., "extract the dataset and evaluation metrics"). The tool first fetches the page content using Jina Reader (Jina.ai, 2025) and then employs Qwen3 (Yang et al., 2025) to synthesize a precise answer based on the goal. This allows for focused knowledge extraction from web pages.
- **Code:** Provides a sandboxed Python environment for computational analysis and verification. It is equipped with standard scientific libraries (e.g., NumPy, SciPy) and allows the agent to execute code for tasks like data analysis or simulations. All outputs (stdout, stderr, and figures) are captured as text, providing empirical evidence for the agent’s reasoning process.

D.4 TRAINING DETAILS

CPT Objective. The continued pre-training (CPT) stage minimizes the standard language modeling loss:

$$\mathcal{L}_{\text{CPT}}(\theta) = - \sum_{t=1}^T \log p_{\theta}(x_t \mid x_{<t}), \quad (1)$$

where x_t denotes the token at position t , and θ are the model parameters.

RFT Objective. The rejection sampling fine-tuning (RFT) stage trains the model on accepted research trajectories. Formally, given a research question $q^{(i)}$, the model generates the reasoning report $r_j^{(i)}$ at round j conditioned on the previous report–observation pair $\{r_{j-1}^{(i)}, o_{j-1}^{(i)}\}$, with initialization $r_0^{(i)} = o_0^{(i)} = \emptyset$. For a collection of K accepted trajectories, where trajectory i has L_i rounds, the objective reduces to supervised learning that maximizes the conditional log-likelihood:

$$\mathcal{L}_{\text{RFT}}(\theta) = - \sum_{i=1}^K \sum_{j=1}^{L_i} \log p_{\theta}\left(r_j^{(i)} \mid q^{(i)}, r_{j-1}^{(i)}, o_{j-1}^{(i)}\right), \quad (2)$$

where θ denotes the model parameters. The loss computed is exclusively on the reasoning report tokens; tool observations are included in the context but excluded from backpropagation.

Implementation. We implement supervised fine-tuning (SFT) using the Megatron-LM framework (Shoeybi et al., 2019). The hyperparameters for fine-tuning our MoE and Dense models are detailed in Table 9 and Table 10, respectively.

D.5 ABLATION ON FINE-TUNING DATASETS

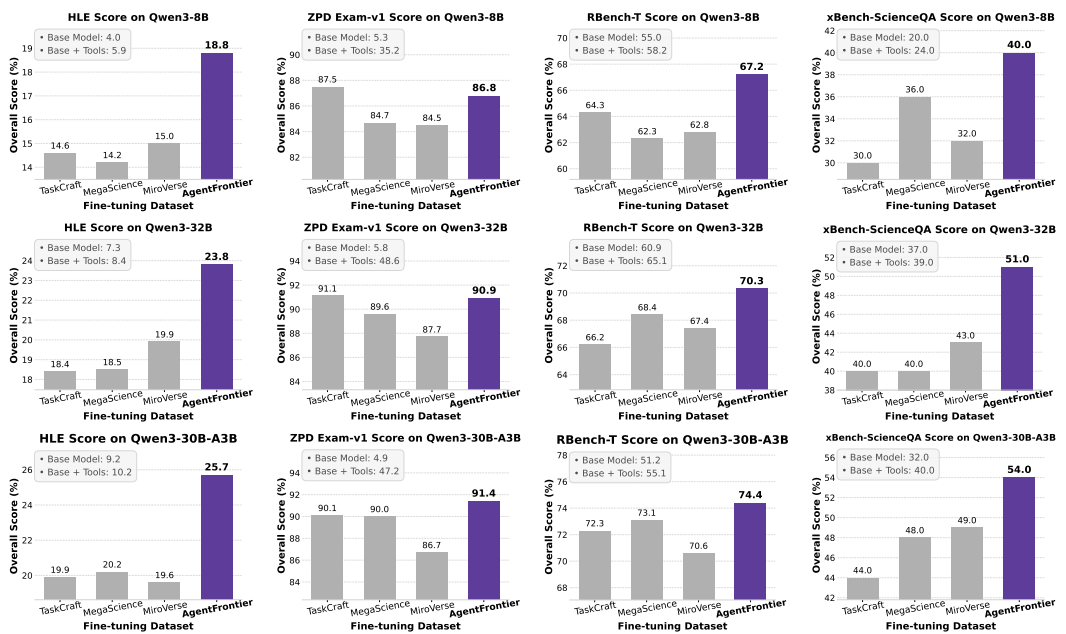
Figure 8 presents an ablation study on the impact of different fine-tuning datasets (TaskCraft, Mega-Science, MiroVerse, and our proposed AgentFrontier data) on the performance of Qwen3-8B and Qwen3-32B models. The results, plotted across all four evaluation benchmarks, show that models fine-tuned with our RFT data almost achieve superior performance, highlighting the effectiveness of our data synthesis strategy.

Table 11 presents a detailed analysis of tool usage and conditional accuracy for Qwen3-30B-A3B model after undergoing rejection-sampling fine-tuning (RFT) on four distinct datasets. The results clearly demonstrate the effectiveness of our synthesized dataset, AgentFrontier. The agent fine-tuned on AgentFrontier achieves the highest overall conditional accuracy on both the ZPD-Exam (87.6%) and RBench-T (63.7%) benchmarks. Furthermore, it consistently secures top-tier accuracy for critical tools across various benchmarks, such as for the Scholar (91.7%) and Brower (91.8%)

1188
1189
1190
1191 Table 9: SFT Hyperparameters for the MoE
1192 Model.

Parameter	Value
Training Epochs	3
Max Sequence Length	40,960
Batch Size	256
Learning Rate	7.0×10^{-6}
Learning Rate (Min)	7.0×10^{-7}
LR Scheduler	Linear Decay
Tensor Parallel (MP)	4
Expert Parallel (EP)	2
Pipeline Parallel (PP)	1

1205 tools on ZPD-Exam and the Code tool on both ZPD-Exam (83.3%) and RBench-T (78.6%). This
1206 superior performance underscores the quality of AgentFrontier in enhancing an agent’s capability to
1207 correctly and robustly utilize tools across a diverse range of complex tasks.

1231
1232 Figure 8: Impact of different fine-tuning datasets on the performance of Qwen3-8B (top row),
1233 Qwen3-32B (mid row), and Qwen3-30B-A3B (bottom row) across four evaluation benchmarks.1234
1235
1236
1237 D.6 CPT RESULTS AND COMPARISONS
1238

1239 Table 12 provides a comprehensive comparison of our model, AgentFrontier-30B-A3B, with state-
1240 of-the-art proprietary and open-source models on the four evaluation benchmarks. We report results
1241 for models with and without tool access. The final rows highlight the performance of our model and
quantify the significant gains achieved through the Continued Pre-training (CPT) stage.

1188
1189
1190
1191 Table 10: SFT Hyperparameters for the
1192 Dense Model.

Parameter	Value
Training Epochs	3
Max Sequence Length	40,960
Batch Size	64
Learning Rate	4.0×10^{-5}
LR Scheduler	Cosine Decay
Warmup Ratio	0.1

Table 11: Tool usage statistics for the Qwen3-30B-A3B agent on the ZPD Exam, RBench-T and xBench-ScienceQA. Each column block shows performance after RFT on a different dataset. We report average usage per round and conditional tool accuracy (Acc, %), defined as the success rate for tasks that use the tool. The final row details overall metrics. Best results are in **bold**.

Fine-tuning Dataset		TaskCraft		MegaScience		MiroVerse		AgentFrontier	
Benchmark	Tool / Metric	Usage	Acc (%)	Usage	Acc (%)	Usage	Acc (%)	Usage	Acc (%)
HLE	Search	0.68	19.6	0.67	20.3	0.73	20.4	0.73	24.9
	Scholar	0.78	21.0	0.98	20.3	0.87	20.6	0.89	25.4
	Browser	1.24	25.2	1.39	23.4	1.47	22.7	1.32	29.8
	Code	0.52	18.1	0.65	18.6	0.67	18.4	0.63	24.9
	Overall (Rounds/Acc.)	4.21	21.0	4.70	20.6	4.74	20.5	4.57	26.3
ZPD-Exam	Search	0.15	90.8	0.10	85.4	0.18	74.8	0.13	83.6
	Scholar	1.20	90.1	1.28	90.2	1.22	87.3	1.23	91.7
	Browser	1.39	90.6	1.35	91.0	1.46	86.9	1.45	91.8
	Code	0.03	78.1	0.03	68.6	0.02	66.7	0.04	83.3
	Overall (Rounds/Acc.)	3.77	87.4	3.76	83.8	3.88	78.9	3.84	87.6
RBench-T	Search	0.23	55.0	0.24	53.6	0.26	50.0	0.28	58.1
	Scholar	0.14	63.1	0.15	59.6	0.16	54.8	0.16	59.7
	Browser	0.20	54.4	0.22	53.8	0.28	46.9	0.27	58.2
	Code	0.74	77.5	0.80	78.6	0.83	77.2	0.88	78.6
	Overall (Rounds/Acc.)	2.31	62.5	2.41	61.4	2.53	57.2	2.59	63.7
xBench-SciQA	Search	0.44	28.6	0.39	50.0	0.36	46.4	0.43	57.1
	Scholar	0.29	54.2	0.39	44.8	0.36	66.7	0.28	48.1
	Browser	0.46	31.6	0.61	38.5	0.48	52.4	0.36	42.1
	Code	0.62	47.2	0.54	46.8	0.60	42.6	0.58	55.6
	Overall (Rounds/Acc.)	2.81	40.4	2.93	45.0	2.81	52.0	2.66	50.7

Table 12: Comparison of AgentFrontier with state-of-the-art proprietary and open-source LLMs/Agents on four high-level multi-disciplinary benchmarks. [†] marks the result from the corresponding official reports. The final row highlights the performance gain from our Continued Pre-training (CPT) stage.

LLMs/Agents	Tools	HLE (text-only)	ZPD Exam-v1	RBench-T	xBench-ScienceQA
<i>Direct Inference (with and without Tools)</i>					
GPT-4o	✗	2.3	4.8	42.0	13.0
	✓	4.8	51.3	48.5	15.0
Claude 4 Sonnet	✗	5.4	6.0	61.8	32.0
	✓	14.3	86.6	71.1	47.0
Gemini 2.5 Flash	✗	10.4	6.3	65.2	35.0
	✓	12.6	58.1	75.8	39.0
DeepSeek V3.1-671B	✗	18.5	8.2	76.3	40.0
	✓	29.8 [†]	<u>93.1</u>	79.4	<u>55.0</u>
Qwen3-30B-A3B (Thinking-2507)	✗	9.2	4.9	51.2	32.0
	✓	10.2	47.2	55.1	40.0
<i>Proprietary Research Agents</i>					
OpenAI DeepResearch	✓	26.6 [†]	–	–	–
Gemini DeepResearch	✓	26.9 [†]	–	–	–
Kimi-Researcher	✓	26.9 [†]	–	–	–
<i>Open-source Agents</i>					
WebDancer-QwQ-32B	✓	6.4	51.8	67.6	38.0
WebSailor-72B	✓	9.2	62.1	44.9	27.0
WebShaper-72B	✓	8.0	54.4	66.8	29.0
<i>Ours</i>					
AgentFrontier-30B-A3B (RFT only)	✓	25.7	91.4	74.4	54.0
AgentFrontier-30B-A3B (CPT+RFT)	✓	28.6	93.4	<u>77.1</u>	61.0
Δ (CPT gain)		+2.9	+2.0	+2.7	+7.0

1296 **D.7 ABLATION STUDY ON THE ZPD CALIBRATION POLICY**
12971298 To isolate the impact of our ZPD-calibration policy, we conduct an ablation study. This exper-
1299 iment directly compares our ZPD-based data selection against a random sampling baseline, to verify
1300 that the performance gains are attributable to our targeted calibration strategy rather than a simpler
1301 sampling heuristic.1302
1303 **Experimental Setup.** We fine-tune three models of varying scales (Qwen3-8B, Qwen3-32B, and
1304 Qwen3-30B-A3B) on 12,000 trajectories sampled from D_{refined} . The experiment compares two con-
1305 ditions, differing only in data selection method: (1) **ZPD Selection (Ours):** Selecting trajectories
1306 via our proposed ZPD-calibration policy. (2) **Random Selection (Baseline):** Randomly sampling
1307 an equal number of trajectories from the same pool, D_{refined} .1308
1309 **Results and Analysis.** The results, presented in Table 13, show that our ZPD-calibration policy.
1310 Across all model scales and evaluation benchmarks, fine-tuning on data selected via our ZPD pol-
1311 icy consistently and significantly outperforms the random baseline. The most substantial gains are
1312 observed on HLE and xBench-SciQA, with improvements of up to +10.0 points. These benchmarks
1313 are specifically designed to evaluate deep, multi-step reasoning. This result strongly suggests that
1314 our ZPD-based mechanism is not merely a difficulty filter, but a targeted strategy that prioritizes tra-
1315 jectories fostering complex reasoning and knowledge fusion—the core capabilities our work aims
1316 to enhance.1316 Table 13: Ablation study comparing our ZPD-based data selection against a random sampling base-
1317 line. Models are fine-tuned on 12,000 trajectories from D_{refined} . Scores are reported on four bench-
1318 marks, with the performance delta over the baseline shown in parentheses. Best results are in **bold**.
1319

Base Model	Data Selection	HLE	ZPD Exam-v1	RBench-T	xBench-SciQA
Qwen3-8B	Random Selection	16.9	85.1	66.1	33.0
	ZPD Selection (Ours)	18.8 (+1.9)	86.8 (+1.7)	67.2 (+1.1)	40.0 (+7.0)
Qwen3-32B	Random Selection	20.9	88.0	69.5	45.0
	ZPD Selection (Ours)	23.8 (+2.9)	90.9 (+2.9)	70.3 (+0.8)	51.0 (+6.0)
Qwen3-30B-A3B	Random Selection	20.9	89.1	72.2	44.0
	ZPD Selection (Ours)	25.7 (+4.8)	91.4 (+2.3)	74.4 (+2.2)	54.0 (+10.0)

1328
1329 **D.8 HYPERPARAMETER SENSITIVITY ANALYSIS**
13301331 This section analyzes the sensitivity of two key hyperparameters in our data synthesis pipeline: the
1332 Best-of-N (BoN) verification attempts, N , and the redundancy threshold, ϵ . Our analysis validates
1333 the chosen values by examining the trade-offs among data quality, yield, and computational cost.1334
1335 **D.8.1 BEST-OF-N VERIFICATION ATTEMPTS (N)**1336 The hyperparameter N for Best-of-N (BoN) verification controls the] trade-off between **data yield**
1337 and **computational cost**. While a higher N increases the chance of verifying a difficult problem
1338 (thus increasing yield), the cost scales linearly with N . We quantify this by testing $N \in [1, 8]$ on
1339 1,000 candidate QA pairs. The results are presented in Table 14.1341 Table 14: Sensitivity analysis for the Best-of-N hyperparameter N . We observe diminishing returns
1342 in pass@N as N increases, while the cost scales linearly. $N = 3$ is identified as the optimal elbow
1343 point, maximizing the gain in yield for the incurred computational cost.

N	1	2	3	4	5	6	7	8
pass@N (%)	29.5	36.0	40.0	43.2	45.1	46.8	48.2	48.9
Marginal Gain (%)	–	+6.5	+4.0	+3.2	+1.9	+1.7	+1.4	+0.7
Relative Cost	1×	2×	3×	4×	5×	6×	7×	8×

1350 As shown in Table 14, the results demonstrate a clear pattern of **diminishing returns**. The yield
 1351 (pass@N) grows substantially up to $N = 3$ (a 10.5% absolute gain), but the marginal gain shrinks
 1352 sharply thereafter. For instance, increasing N from 4 to 8 only yields an additional 5.7% of data at
 1353 double the cost. We therefore identify $N = 3$ as the **optimal elbow point**. This value strikes an
 1354 effective balance between high data yield and acceptable computational cost.
 1355

1356 D.8.2 REDUNDANCY THRESHOLD (ϵ)

1357 The redundancy threshold, ϵ , balances **dataset diversity** against **data volume**. We chose $\epsilon = 0.7$
 1358 based on both quantitative analysis and qualitative inspection.
 1359

1360 Table 15: Cumulative percentage of data retained as a function of the similarity threshold ϵ . Setting
 1361 $\epsilon = 0.7$ filters approximately 30% of the most similar pairs while retaining 70% of the data, striking
 1362 a balance between diversity and volume.
 1363

1364 Threshold (ϵ)	0.1	0.2	0.3	0.4	0.5	0.6	0.7	0.8	0.9
1365 Retained Data (%)	5.12	13.94	24.55	36.29	48.50	59.20	70.42	81.69	93.43

1367
 1368
 1369 **Quantitative Analysis** Setting $\epsilon = 0.7$ retains approximately 70% of the data while filtering the
 1370 ~30% of pairs most likely to be redundant. As Table 15 shows, a lower threshold (e.g., $\epsilon < 0.7$)
 1371 would significantly reduce data volume, whereas a higher one (e.g., $\epsilon > 0.7$) would be less effective
 1372 at enhancing diversity.
 1373

1374 **Qualitative Analysis** To validate this threshold, we qualitatively inspected pairs with similarity
 1375 scores around 0.7. We find it serves as an effective semantic cutoff, distinguishing semantically
 1376 redundant paraphrases from complementary reasoning problems.
 1377

1378 **Case 1: Redundant (Score = 0.796 > ϵ)** These two questions are essentially paraphrases that
 1379 target the same core concept, offering little additional training value.
 1380

QA-pair 1:

Question: What property of the partially ordered set of
 equivalence classes of subsets of the rationals under
 homeomorphic embeddability guarantees the absence of both
 infinite antichains and infinite strictly decreasing chains?

Answer: partially well-ordered

QA-pair 2:

Question: For equivalence classes of subsets of \mathbb{Q} under
 topological embeddability, what binary relation defines the
 partial order between distinct equivalence classes [A] and
 [B] in the poset structure?

Answer: homeomorphic embeddability

Similarity: 0.796

1395 **Case 2: Complementary (Score = 0.707 $\approx \epsilon$)** In contrast, these questions probe different facets
 1396 (a character vs. the underlying principles) of the same scenario, offering complementary training
 1397 value.
 1398

QA-pair 1:

Question: In a 1993 meta-cinematic work, which character's
 decision to abort a bicycle stunt--after calculating
 97.3% fatality probability through narrative role
 analysis--demonstrates correct application of the formula
 $F\Delta t = m\Delta v$ to avoid momentum conservation violations?

Answer: Danny Madigan

1404 QA-pair 2:
 1405 Question: In Last Action Hero's bicycle stunt scene, Danny
 1406 Madigan's abort decision combines which three elements: (1)
 1407 a narrative trope realization about his character role, (2)
 1408 implicit application of a momentum conservation principle,
 1409 and (3) avoidance of a high-probability negative outcome
 1410 derived from collision physics?
 1411 Answer: comedy sidekick, impulse-momentum theorem, fatal
 1412 trauma
 1413 Similarity: 0.707

1414 In summary, our choice of $\epsilon = 0.7$ is empirically justified, balancing dataset diversity and volume
 1415 to ensure the final training set is rich in novel reasoning challenges.

1417 E CASE STUDY

1419 Clinical Scenario from Humanity's Last Exam

1421 **Question:** A 68 year old patient presents to your clinic with ankle pain and swelling. The
 1422 swelling began after a long walk with his wife the previous day. Physical exam shows
 1423 erythema, slight edema, and pain on flexion and extension as well as mild bony tenderness.
 1424 X-rays are negative for any acute abnormality. The patient is treated with indomethacin. He
 1425 returns to the clinic 10 days later with the same pain, swelling, and redness. Laboratory
 1426 workup reveals a slightly elevated uric acid and C-reactive protein. X-rays once again rule
 1427 out any acute findings. The patient is treated with a prednisone taper, but his symptoms
 1428 begin to worsen. Joint aspiration and synovial fluid analysis reveals no crystals and gram
 1429 stain reveals no organisms or white blood cells. What is this patient's diagnosis?

1431 **Ground Truth Diagnosis: Chronic osteomyelitis**

1435 ✖ OpenAI DeepResearch Output (Incorrect)

1436 Based on the clinical presentation and diagnostic findings, this patient's most likely diagnosis is **Charcot Arthropathy**. Here's the reasoning:

- 1439 1. Chronic and Recurrent Swelling with Erythema: Charcot arthropathy often presents
 1440 with recurrent swelling, warmth, and erythema, which can be mistaken for infections or inflammatory arthritis.
- 1442 2. X-rays Negative for Acute Findings: Early Charcot arthropathy may not show significant abnormalities on X-rays, though later stages may demonstrate joint destruction or deformity.
- 1445 3. Joint Aspiration Findings: The absence of crystals (ruling out gout or pseudogout) and no organisms or WBCs (ruling out septic arthritis) suggests a non-infectious etiology.
- 1448 4. Risk Factors: This is commonly associated with diabetes mellitus or other neuropathic conditions, which should be explored in this patient.

1450 *Research completed in 10m · 20 sources · 75 searches*

1451 **Why Charcot Arthropathy Fits Best**

1452 Several clinical clues in this case strongly support Charcot neuropathic arthropathy as the
 1453 correct diagnosis:

- 1454 • **Normal X-rays despite severe symptoms:** In early Charcot arthropathy (Stage 0),
 1455 patients have an acutely inflamed joint before any bony destruction is visible on
 1456 radiographs. This patient's X-ray showed no acute abnormalities even though his
 1457 ankle was red, hot, and swollen – a classic scenario for early Charcot changes...

1458

1459

1460

1461

1462

1463

1464

1465

1466

1467

1468

1469

1470

1471

1472

1473

1474

1475

1476

1477

1478

1479

1480

1481

1482

1483

1484

1485

1486

1487

1488

1489

1490

1491

1492

1493

1494

1495

1496

1497

1498

1499

1500

1501

1502

1503

1504

1505

1506

1507

1508

1509

1510

1511

- **Peripheral neuropathy signs and risk factors:** Charcot arthropathy virtually always occurs in the setting of neuropathy. Although not explicitly stated, a 68-year-old patient is likely to have neuropathy...
- **Laboratory and fluid studies exclude other causes:** The synovial fluid had **no crystals, no organisms, and minimal inflammatory cells**, which is exactly what one might find in Charcot...
- **Episode triggered by activity (trauma):** The history that symptoms recur “following activity” aligns with Charcot pathogenesis. Episodes often start after minor trauma or increased weight-bearing exercise...
- **Initial improvement with NSAIDs, then worsening on steroids:** In Charcot arthropathy, treating with just anti-inflammatories can temporarily reduce swelling and pain, but if the patient continues to walk on the joint, the underlying bony collapse progresses...

In summary, the constellation of a relatively **painless, swollen red ankle**, with **normal X-rays, negative joint fluid**, and a history of neuropathy or diabetes, is virtually pathognomonic for **Charcot neuropathic arthropathy** once infection and crystals are ruled out. The case matches this picture closely, making Charcot joint the most likely diagnosis.

Sources:

1. Amelia Harris, Melanie Violand. Charcot Neuropathic Osteoarthropathy. StatPearls, 2023
2. Botek G, Hild G. Differential diagnosis of Charcot arthropathy. Lower Extremity Review. 2011
3. Pinzur MS. Charcot foot: clinical clues, diagnostic strategies, and treatment principles. American Family Physician. 2018;97(9):594-600
4. Rosskopf AB, et al. The Charcot foot: a pictorial review. Insights Imaging. 2019;10(1):77
5. Singh D, et al. Diagnosing acute monoarthritis in adults: a practical approach. Am Fam Physician. 2003;68(1):83-90
6. Lower Extremity Review (2011). Charcot arthropathy imaging and management
7. Radiopaedia. Osteoarthritis of the ankle – radiographic features
8. Lower Extremity Review (2011). Charcot foot vs. gout and infection

1566

1567

1568

1569

1570

1571

1572

1573

1574

1575

1576

1577

1578

1579

1580

1581

1582

1583

1584

1585

1586

1587

1588

1589

1590

1591

1592

1593

1594

1595

1596

1597

1598

1599

1600

1601

1602

1603

1604

1605

1606

1607

1608

1609

1610

1611

1612

1613

1614

1615

1616

1617

1618

1619

Round 3: Finalizing Diagnosis

Status Report and Deep Analysis Progress Achieved: The second, more targeted literature search provided crucial confirmatory evidence, allowing for a final synthesis of all findings and a resolution of the remaining diagnostic uncertainties.

- **Synthesized Literature Findings:** The model integrated results from the second tool call to build a robust case for chronic osteomyelitis.

- **Explaining Negative Findings:** The search for "osteomyelitis ankle negative synovial fluid" yielded articles confirming that false negative results in synovial fluid cultures and gram stains are possible, and that "culture-negative osteomyelitis" is a recognized clinical entity. This directly addressed a key uncertainty from Round 1, explaining why a bone infection could be present despite "clean" joint fluid. Similarly, literature confirmed that initial radiographs are often negative in osteomyelitis, validating the patient's repeated negative X-rays.

- **Confirming the Steroid Paradox:** The search on "ankle arthritis steroid exacerbation" reinforced the understanding that corticosteroid use can lead to adverse outcomes. By cross-referencing this with the infectious nature of osteomyelitis, the model concluded that the patient's worsening symptoms were a classic sign of an occult infection being unmasks by immunosuppression, transforming this paradoxical finding into a powerful diagnostic clue.

- **Differentiating from Alternatives:** The search on "tuberculous arthritis ankle presentation" revealed that it typically presents as a subacute or chronic monoarthritis, often over weeks to months. This contrasts with the patient's more acute onset following a specific event (the long walk), making tuberculous arthritis a less likely, though still possible, alternative compared to chronic osteomyelitis.

- **Re-evaluation of Clinical Data:** In light of the new evidence, the model re-evaluated the initial data with greater clarity.

- The **bony tenderness** is now seen as a specific sign of bone involvement, not just generalized joint pain.

- The elevated **C-reactive protein (CRP)** is confirmed as a marker of significant inflammation, consistent with a bone infection.

- The slightly elevated **uric acid** is confidently dismissed as a non-specific finding or a red herring, as no other evidence supports a diagnosis of gout.

- **Diagnostic Certainty Assessment:** The model's confidence in the diagnosis of Chronic Osteomyelitis increased substantially. All other possible diseases had been systematically ruled out by clinical data. Chronic Osteomyelitis remained the only diagnosis that could cohesively explain the entire constellation of findings: persistent symptoms, bony tenderness, negative initial imaging and fluid analysis, and the critical paradoxical response to steroid therapy. The supporting literature provided a solid foundation for this conclusion.

Next Steps Plan: No further investigation is required. The diagnostic pathway has been conclusively established through systematic elimination of alternatives and the integration of clinical findings with targeted, confirmatory literature evidence. The available information is sufficient to provide a definitive diagnosis.

1620

1621

1622

1623

1624

1625

1626

1627

1628

1629

1630

1631

1632

1633

1634

1635

1636

1637

1638

1639

1640

1641

1642

1643

1644

1645

1646

1647

1648

1649

1650

1651

1652

1653

1654

1655

1656

1657

1658

1659

1660

1661

1662

1663

1664

1665

1666

1667

1668

1669

1670

1671

1672

1673

Final Answer and Clinical Reasoning

Based on the comprehensive clinical evaluation and integration of supporting literature evidence, this patient's diagnosis is **Chronic Osteomyelitis**.

DIAGNOSTIC PROCESS

The diagnostic journey for this 68-year-old patient began with acute ankle pain and swelling... The most critical diagnostic turning point came with the synovial fluid analysis... combined with the patient's paradoxical worsening during prednisone therapy...

DIFFERENTIAL DIAGNOSIS ELIMINATION

Through systematic exclusion of alternative diagnoses, chronic osteomyelitis emerges as the most consistent explanation...

PATHOPHYSIOLOGICAL MECHANISMS SUPPORTING CHRONIC OSTEOMYELITIS

Chronic osteomyelitis provides the most coherent explanation for this clinical scenario through several key mechanisms:

Insidious Presentation with Normal Radiographs Chronic osteomyelitis often presents with minimal early radiographic changes...

Paradoxical Response to Steroids The worsening during prednisone therapy is particularly telling. Corticosteroids suppress the immune system, allowing previously contained bacterial colonies within necrotic bone to proliferate unchecked...

Synovial Fluid Findings The negative synovial fluid analysis does not exclude osteomyelitis, as the infection originates in the bone marrow...

Bony Tenderness Without Acute Trauma The mild bony tenderness... indicates underlying bone pathology consistent with osteomyelitis...

SUPPORTING EVIDENCE FROM LITERATURE

Recent medical literature corroborates this diagnostic conclusion. Studies indicate that chronic osteomyelitis of the foot and ankle frequently presents with challenging diagnostic features... The paradoxical worsening with corticosteroid therapy aligns perfectly with the known pathophysiology...

CONCLUSION

In summary, this patient's clinical presentation—characterized by acute inflammatory symptoms, normal radiographs, negative synovial fluid analysis, and paradoxical worsening with steroid therapy—best aligns with chronic osteomyelitis rather than any of the other listed conditions...

1674 F PROMPTS USED IN EXPERIMENTS
1675
1676
16771678 The key prompts used in our experiments are presented below to ensure reproducibility.
1679
1680
1681
1682
1683

F.1 EVALUATION PROMPT

1684 **Evaluation Prompt**
16851686 Judge whether the following [response] to [question] is correct or not based on the
1687 precise and unambiguous [correct_answer] below.
16881689 **[question]:** {question}
1690 **[response]:** {response}1691 Your judgement must be in the format and criteria specified below:
16921693 **extracted_final_answer:** The final exact answer extracted from the
1694 [response]. Put the extracted answer as 'None' if there is no exact,
1695 final answer to extract from the response.1696 **[correct_answer]:** {correct_answer}1697 **reasoning:** Explain why the extracted_final_answer is correct or incorrect
1698 based on [correct_answer], focusing only on if there are meaningful differ-
1699 ences between [correct_answer] and the extracted_final_answer.
1700 Do not comment on any background to the problem, do not attempt to solve the
1701 problem, do not argue for any answer different than [correct_answer], focus
1702 only on whether the answers match.1703 **correct:** Answer 'yes' if extracted_final_answer matches the
1704 [correct_answer] given above, or is within a small margin of error for
1705 numerical problems. Answer 'no' otherwise, i.e. if there is any
1706 inconsistency, ambiguity, non-equivalency, or if the extracted answer is incorrect.1707 **confidence:** The extracted confidence score between 0% and 100% from
1708 [response]. Put 100 if there is no confidence score available.
17091710
1711
1712 F.2 SIMILARITY FILTER PROMPT
1713
17141715 **Similarity Filter Prompt**
17161717 Determine if the candidate QA pair expresses **EXACTLY** the same specific question and
1718 answer as the reference QA pair.
17191720 **Requirements:**1721 1. The question must ask for identical information with identical technical require-
1722 ments.
1723 2. The answer must provide identical content with identical technical details.
1724 3. Any difference in the specific information requested or provided means they are
1725 NOT identical.
1726 4. Pay special attention to mathematical expressions, symbols, and technical specifi-
1727 cations.

1728
1729

F.3 AGENTIC REFINEMENT PROMPT

1730
1731**Prompt for Agentic Refinement ($\mathcal{A}_{\text{refine}}$)**

1732

Role and Objective:1733
1734
1735
1736

You are a sophisticated agent tasked with iterative data refinement. Your primary mission is to transform a given Question-Answer pair (q_k, a_k) into a more complex, in-depth, and factually grounded pair (q_{k+1}, a_{k+1}) . This escalation must be achieved by leveraging a specialized tool suite $\mathcal{T} = \{T_{\text{search}}, T_{\text{scholar}}, T_{\text{browser}}, T_{\text{code}}\}$.

1737

Input:

1738

The current QA pair QA pair (q_k, a_k) in a structured format.

1739

Mandatory Refinement Protocol:1740
1741
1742

Your task is to generate a new, superior QA pair by applying one or more of the following four refinement dimensions. For each generated pair, you **must** utilize the provided tools and explicitly log their usage.

1743

1. **Knowledge Expansion:**

1744

- **Objective:** Broaden the informational scope of the QA pair.
- **Action:** You **must** use the T_{search} , T_{scholar} , or T_{browser} tools to discover and retrieve relevant background knowledge, historical context, or contrasting perspectives.
- **Implementation:** Weave this new information seamlessly into the refined question (q_{k+1}) and provide a comprehensive explanation in the refined answer (a_{k+1}) .

1745

2. **Conceptual Abstraction:**

1746

- **Objective:** Elevate the level of abstract reasoning required.
- **Action:** Analyze the core concepts within (q_k, a_k) . Formulate a new question (q_{k+1}) that requires identifying higher-level principles, synthesizing information to uncover subtle relationships, or drawing non-obvious analogies.
- **Implementation:** The refined answer (a_{k+1}) must explicitly articulate this abstract principle or relationship. You may use T_{scholar} to find established theoretical frameworks to aid this process.

1747

3. **Factual Grounding:**

1748

- **Objective:** Enhance the factual accuracy, precision, and verifiability.
- **Action:** You **must** use T_{search} and T_{scholar} to perform multi-source cross-validation of the facts and claims in a_k .
- **Implementation:** Augment the refined answer (a_{k+1}) with precise quantitative data, specific named entities, and direct citations or references to the authoritative sources you retrieved.

1749

4. **Computational Formulation:**

1750

- **Objective:** Introduce a verifiable computational or logical reasoning challenge.
- **Action:** You **must** use the T_{code} tool (a Python execution environment) to design a new question (q_{k+1}) that necessitates a quantitative calculation or algorithmic simulation.
- **Implementation:** The refined answer (a_{k+1}) must contain: (1) The complete, executable Python code block used to solve the problem, and (2) The final output produced by the code, along with a brief explanation.

1751

Tool Usage Protocol: {tools}

1752

Final Instruction:

1753

Proceed with the refinement of the provided (q_k, a_k) . Your response must be only the final JSON object.

1754

1755

1756

1757

1758

1759

1760

1761

1762

1763

1764

1765

1766

1767

1768

1769

1770

1771

1772

1773

1774

1775

1776

1777

1778

1779

1780

1781